Semiconductor heterostructures

Zh. I. Alferov, V. M. Andreev, and N. N. Ledentsov

Introduction

It is impossible to imagine now the modern solid state physics without semiconductor heterostructures. Semiconductor heterostructures and, particularly, double heterostructures including quantum wells (QWs), quantum wires (QWRs), and quantum dots (QDs) are today the subject of research of 2/3 of the semiconductor physics community.

While the possibility of controlling the type of conductivity of a semiconductor material by doping with various impurities and the idea of injecting nonequilibrium charge carriers were the seeds from which semiconductor electronics had evolved, heterostructures made it possible to solve a much more general problem of controlling the fundamental parameters of semiconductor crystals and devices: band gaps, effective masses and mobilities of charge carriers, refractive indices, electronic band structure, etc.

The development of the physics and technology of semiconductor heterostructures has resulted in remarkable changes in our everyday life. Heterostructure electronics is widely used in many areas of human civilization. It is hardly possible to imagine our life without double heterostructure (DHS) laser-based telecommunication systems, heterostructure light-emitting diodes, heterostructure bipolar transistors, and low-noise high electron mobility transistor (HEMT) for high frequency applications including, for example, satellite television. DHS laser enters now practically every house with CD-players. Heterostructure solar cells have been widely used for space and terrestrial applications— *Mir* space-station has been using AlGaAs heterostructure solar cells for nearly 10 years.

Historical prerequisites for the appearance of heterostructures

Systematic studies of semiconductors were started in the early 1930s at the Physico-Technical Institute under the direct leadership of its founder—Abram F. Ioffe. V. Zhuze and B. Kurchatov studied the intrinsic and impurity conductivity of semiconductors in 1932 [1]. In the same year, A. Ioffe and Ya. Frenkel created the theory of rectification in the metal-semiconductor contact based on the tunneling phenomenon [2]. In 1931 and 1936, Ya. Frenkel published his famous articles [3,4,5] where he predicted exciton effects, gave a name to the phenomenon, and developed a theory of excitons in semiconductors. E. Gross experimentally discovered excitons in 1951 [6,7]. The first diffusion theory of a rectifying p-n heterojunction, which laid foundation for W. Shockley's p-n junction theory, was published by B. Davydov in 1939 [8]. By A. Ioffe's initiative, research into intermetallic compounds was started at the Physico-Technical Institute in the late 1940s. Semiconducting properties of $A_{III}B_{V}$ compounds were independently predicted theoretically and discovered experimentally by H. Welker [9,10] and N. Goryunova and A. Regel at the Physico-Technical Institute [11,12]. The high theoretical, technological, and experimental level in this area, which had already existed at the Institute by that time, served as a basis for further work.

The concept of using heterojunctions in semiconductor electronics had already been put forward at the very dawn of electronics era. Already in his first patent concerned with p-n-junction transistors W. Shockley [13] proposed a wide-gap emitter to obtain unidirectional injection. A. Gubanov in the Institute was the first to analyze theoretically current–voltage characteristics of isotype and anisotype heterojunctions [14,15], but one of the most important theoretical investigations at this early stage of heterostructure research was done by H. Kroemer, who introduced the concept of quasi-electric and quasi-magnetic fields in a graded heterojunction and made an assumption that heterojunctions might exhibit extremely high injection efficiencies in comparison to homojunctions [16,17]. In the same period, various concepts were developed regarding application of heterostructures in semiconductor solar cells.

A next important step was made several years later when the concept of double heterostructure lasers was formulated independently by Zh. Alferov and R. Kazarinov [18] and H. Kroemer [19]. In patent [18] the possibility of achieving high density of injected carriers and inverse population by "double" injection was outlined. It was pointed out that homojunction lasers "do not provide CW generation at elevated temperatures" and considered the possibility "to enlarge the emitting surface and use new materials in various spectral regions" to be an additional advantage of DHS lasers.

In his article, H. Kroemer proposed to use DHS for carrier confinement in the active region. He suggested that "lasing can be obtained in quite a number of indirect gap semiconductors and improved in direct gap ones with the use of a pair of heterojunction injectors".

Initially theories were developed much faster than realized experimentally. In 1966, Zh. Alferov with co-workers predicted that the density of injected carriers could be several orders of magnitude higher than the carrier density in the wide-gap emitter ("superinjection" effect) [20]. The same year, in a paper [21] submitted to a new Soviet Journal *Fizika i Tekhnika Poluprovodnikov* (English translation: Sov. Phys. Semiconductors) the authors summarized their understanding of the main advantages of the DHS for use in different devices, especially lasers and high power rectifiers:

"The regions of recombination, light emission, and population inversion coincide, being concentrated in the central layer. Owing to potential barriers at interfaces between semiconductors with forbidden bands of different width, through leakage currents of electrons and holes are completely absent, even under strong forward bias, and there is no recombination in the emitters (in contrast to p-i-n, p-n-n^+, n-p-p^+ homostructures in which recombination plays the key role).

The population inversion can be achieved for obtaining stimulated emission by purely injection method (double injection), and there is no necessity for high doping level of the central region ordegenerate doping. Because of a considerable difference between the dielectric constants, the light is completely concentrated in the central layer which acts as an effective waveguide, and thus there is no light loss in the passive regions (emitters)."

Here are the most important features of semiconductor heterostructures were underlined at that time:

- Superinjection of carriers
- Optical confinement
- Electron confinement.

Then it only remained to find a heterostructure in which these phenomena could be realized.

At that time, general skepticism existed in respect to the possibility of creating the "ideal" heterojunction with defect-free interface and, all the more, the theoretically predicted injection properties. Even the pioneering study of the first lattice-matched epitaxial single-crystal Ge-GaAs heterojunctions by R. Anderson [22,23] gave no proof of nonequilibrium carrier injection in heterostructures. Actual realization of the efficient wide-gap emitters was considered nearly impossible and the double heterostructure laser patent was often referred to as a "schreibtisch patent."

Mostly owing to this general skepticism, only few groups had been trying to find an "ideal couple," which was, naturally, a difficult problem. Many conditions of compatibility between thermal, electrical, and crystallochemical properties and between the crystal and band structure of the contacting materials are to be met.

A lucky combination of a number of properties, i.e., small effective mass and wide energy gap, effective radiative recombination, sharp optical absorption edge due to "direct" band structure, high electron mobility at the absolute minimum of the conduction band, and its strong reduction at the nearest minimum at the (100) point ensured for GaAs a place of honor in semiconductor physics and electronics even at that time. Since the maximum effect is achieved by using heterojunctions between a semiconductor serving as the active region and a wider band-gap material, the most promising systems considered at that time were GaP-GaAs and

AlAs-GaAs. To be "compatible," materials of the "couple" must have, as the first and the most important condition, close lattice constants; therefore, heterojunctions in the system AlAs-GaAs were preferable. However, prior to starting the work on preparation and study of these heterojunctions, one had to overcome a certain psychological barrier. By that time, AlAs had long been synthesized, but many properties of this compound remained poorly studied, since AlAs was known to be chemically unstable and to decompose in moist air. The possibility of preparing stable and applicable heterojunctions in this system seemed to be not very promising.

Initially, the attempts to create DHS were related to a lattice-mismatched GaAsP system. Zh. Alferov *et al.* succeeded in fabricating by vapor phase epitaxy (VPE) first DHS lasers in this system. However, owing to lattice mismatch, the lasing occurs only at liquid nitrogen temperature, similarly to homojunction lasers [24]. Curiously, this was the first practical result obtained for a lattice-mismatched, even part relaxed system.

This experience, gained in studying the GaAsP system, was very important for understanding many specific physical properties of heterojunctions and basics of heteroepitaxy. The development of the multichamber VPE method for GaAsP system permitted to create in 1970 superlattice structures with a 200-Å period and to demonstrate the splitting of the conduction band [25].

However, by the end of 1966, Zh. Alferov and co-workers came to a conclusion that even the small lattice mismatch in $GaP_{0.15}As_{0.85}$-GaAs heterostructures gives no way of realizing the potential advantages of the DHS. At that time, D. Tret'yakov found out that nothing happened to small crystals of $Al_xGa_{1-x}As$ solid solutions of different compositions, which had been prepared two years before by cooling from a melt and put in a desk drawer by A. Borshchevskii. It immediately became clear that $Al_xGa_{1-x}As$ solid solutions are chemically stable and suitable for preparing durable heterostructures and devices. Studies of the phase diagrams and growth kinetics in this system and the development of a version of the liquid phase epitaxy (LPE) method for heterostructure growth soon resulted in the fabrication of the first lattice-matched AlGaAs heterostructure. When the first paper on this subject was published [26], the authors were lucky to be the first to find out a unique, practically ideal, lattice-matched system for GaAs; but, as it frequently happens, the same results were obtained simultaneously and independently by H. Rupprecht and J. Woodall at T. Watson IBM Research Center [27].

Further progress in the semiconductor heterostructure field was very rapid. First of all Zh. Alferov *et al.* confirmed experimentally the unique injection properties of the wide-gap emitters and the superinjection effect [28], demonstrated stimulated emission in AlGaAs DHS [29], determined the band-diagram of $Al_xGa_{1-x}As$-GaAs heterojunction, and thoroughly studied luminescence properties, carrier diffusion in a graded heterostructure, and very interesting peculiarities of current flow through the heterojunction, e.g., diagonal tunneling-recombination transitions directly between holes from the narrow-band, and electrons from the wide-band heterojunction components [30–33].

At that same time the authors created the majority of most important devices in which the main advantages of heterostructures were realized:

- Low-threshold DHS lasers operating at room temperature [34]
- High-efficiency single heterostructure (SHS) and DHS light emitting diodes (LEDs) [35]
- Heterostructure solar cells [36]
- Heterostructure bipolar transistors [37]
- Heterostructure p-n-p-n thyristor switching devices [38].

Most of these results were reproduced in other laboratories in 1–2 years, and in some cases even later.

Methods of heterostructure fabrication

Heterojunctions are mainly fabricated by epitaxy, producing perfect single crystal layers of the same material as that of the substrate (homoepitaxy) or some other material (heteroepitaxy). In the latter case, it is highly important to match crystal lattice parameters of the material being grown and the base material. Characteristic features making the epitaxy method widely accepted in the semiconductor technology are the following: high perfection of materials being crystallized and possibility of changing the properties of materials over wide limits and varying the layer thickness from a fraction of atomic layer to hundreds of micrometers. Three main epitaxial techniques are being widely used at the Ioffe Institute: liquid phase epitaxy, vapor phase epitaxy, and molecular beam epitaxy.

Liquid phase epitaxy

Owing to its comparative simplicity, LPE has been mainly used for fabricating heterostructures and related devices since the middle 1960s [39]. The driving force of crystallization in this technique is supersaturation of the liquid phase with the material being crystallized. Epitaxial growth of germanium from indium solution was performed in the early 1950s [40]. At the Institute, this method was most fully developed for fabricating power germanium rectifiers [41] with a breakdown voltage of 600 V and working currents of up to 500 A at a device area of up to 3 cm^2. In 1963, the LPE method was used to fabricate p-n junctions in GaAs [42] and then introduced at the Ioffe Institute for the first time to fabricate structures with heterojunctions in the system Al-Ga-As and create on their basis high-voltage diodes [26], LEDs [35], lasers [34], and solar cells [36].

Several modifications of LPE were developed for fabricating multilayer structures with heterojunctions. In one of these, employing a graphite container, multilayer structures are grown by placing alternately one melt after another over the substrate so that several layers of various composition are successively grown on it. This approach has been successfully used at the Ioffe Institute for fabricating multilayer structures based on AlGaAs/GaAs [34–36, 39], InGaAsP/GaAs [43], InGaAs/InP [44], InGaAsSb [45], and other heterojunctions. To grow laser heterostructures with quantum dots in GaInAsP/GaAs and GaInAsP/InP systems, a modified LPE method, in which layer thickness is reduced down to several lattice constants by shortening the time of contact between substrate and melt to 1–10 ms, was proposed and developed [43].

In a piston-type device first developed at the Ioffe Institute [46], melts on the substrate are changed by displacing a preceding melt by the following one which markedly reduces the number of defects at interfaces between layers of different composition and improves the planarity and quality of layers. This technique produced LEDs with efficiency as high as 45% [47]; lasers with QWs in which the threshold current density was reduced to 120 A cm^{-2} at room temperature [48], and solar cells with efficiency >25% at 100–1000 suns [49].

Vapor phase epitaxy

VPE is a technique for epitaxial growth of semiconductor structures including transfer of a mixture of gaseous reagents to the surface of a crystalline substrate with the subsequent growth of layers as a result of chemical reactions between the reagents and the substrate. $A_{III}B_V$ heterostructures are mainly grown at the Ioffe Institute by two modifications of VPE: chloride and metal-organic.

Among the specific features of the chloride technique are sufficiently high growth rates of high-purity and high-mobility undoped gallium arsenide layers $n = 10^{12}$ cm^{-3}, $\mu_{4\ K} = 2.5\times 10^6$ cm^2 V^{-1} s^{-1}. A chloride technique producing multilayer GaAs and GaP structures with heterojunctions was developed at the Ioffe Institute [24,25] and used to fabricate electric energy conversion and luminescent structures: GaAs and GaP_xAs_{1-x} ($0<x><1$) superlattices with separate layer thickness of ~ 10 nm on which conduction band splitting was first observed experimentally [25]; GaP rectifying structures on silicon substrates with working temperatures as high as 450 °C; GaAs diodes, transistors, and thyristors operating at currents of up to 100 A in continuous mode at reverse voltages as high as 2.5 kV and working temperatures of up to 300 °C.

In metal-organic chemical vapor deposition (MOCVD), organometal compounds are used as sources of group III elements and group V elements are delivered at the substrate in the form of hydrides with the subsequent decomposition near the substrate. The main advantage of the MOCVD technique is the relatively simple reactor design which enables obtaining QW heterostructures with abrupt heteroboundaries and steep doping profiles by rapidly changing the vapor phase composition.

Works on MOCVD were commenced at the Ioffe in the late 1970s. Metastable solid solutions in the system Ge-GaAs [50], a rather peculiar example of a crystalline material whose properties are not uniquely determined by its composition and strongly depend on growth conditions, were obtained for the first time in the world. Lasers with threshold current density as low as 80 A cm^{-2} (300 K) were created on the basis of AlGaAs/InGaAs heterostructures with QWs [51]. Also, the concept of a laser on $In_{0.5}Ga_{0.5}As$ QDs built in the GaAs matrix in its turn sandwiched between AlGaAs layers was successfully implemented [52]. Of considerable interest are works on $A_{III}B_V$ heterostructures on Si substrates [53] and AlGaAs/GaAs solar cells [54].

Molecular beam epitaxy

Molecular beam epitaxy (MBE) is the method of epitaxial growth involving a chemical interaction of one or more molecular or atomic beams with the surface of a heated single-crystalline substrate. The source materials are placed in evaporating cells—crucibles made of a high-melting point inert material (e.g., pyrolytic boron nitride) of such dimensions and shape which ensure a uniform flow of atoms or molecules at the substrate surface. Each crucible is enveloped with a resistive heater and protective thermal shields. A substrate is mounted onto a holder ensuring its uniform heating. All MBE machines are equipped with means for obtaining and maintaining ultrahigh vacuum at a level no worse than 10^{-10} torr which is caused by the necessity for minimizing flows of uncontrollable impurities onto the surface. Reflection high-energy electron diffraction (RHEED) allows control over the growth mechanism (amorphous, polycrystalline, or epitaxial) and growth rate, reconstruction of the surface of a growing single-crystalline film, and monitoring any morphological changes occurring in epitaxy.

The results of the initial stage of MBE studies were understood as indicating that this technique is an entirely nonequilibrium process with information about it obtainable only by studying the kinetics of specific reactions.

In view of the desirable use of a broad VPE and LPE experience gained at the Ioffe Institute, the development of a thermodynamic approach to processes occurring in MBE [55,56] was started from the very beginning of MBE studies in 1979–1980.

Gas-phase reactions were considered with account of the equilibrium constants and element activity coefficients known from LPE and VPE, with pressures corresponding to atomic and molecular flows away from the growth surface taken as equilibrium pressures [55]. This is a feature distinguishing the given approach from the thermodynamic description proposed, e.g., in [57] where the ratio of group III and IV atoms arriving at the surface was taken as equilibrium parameter.

This approach allowed describing adequately the MBE growth of binary com-
pounds [55]. Even more dramatic was the success in applying the thermodynamics to describing the segregation of the basic components and impurities conventionally analyzed in MBE as a kinetic process. The model [58] was based on considering phase equilibria in MBE of multicomponent solid solutions and doped layers. For example, it was shown that the abrupt increase in the arsenic equilibrium pressure at the liquidus Ga-Sn-GaAs:Sn is due to the depletion of the liquid phase of gallium and, correspondingly, its enrichment with arsenic. Here, the adequate thermodynamic analysis takes into account quantitatively the appearance of segregated layers of tin and some other features. The thermodynamic approach can explain without invoking the kinetics the existence of a "forbidden" range of AlGaAs growth and suggests ways of overcoming this problem [58]. In the next stage, it was shown that the effects of impurity diffusion in MBE, e.g., the dramatic increase in the beryllium diffusion coefficient in GaAs under certain technological conditions, can also be explained quantitatively on the basis of thermodynamic concepts [59]. Also, the effects of doping [55,60] and the influence of lattice mismatch between the substrate and the growing layer on phase equilibria were considered and the applicability of thermodynamics in this case, too, was demonstrated experimentally by the example of MBE growth of InSb on GaAs and Si [61]. The thermodynamic analysis was also extended to multicomponent solid solutions In-Ga-As-P [62].

Physical processes in heterostructures

Classical heterostructures

The most important results of the development of classical heterostructures can be conveniently categorized as follows.

Realization of ideal DHS leads to the appearance of unique properties and such new fundamental phenomena in the structures (Fig. 1) as:

- One-side injection
- Superinjection
- Diffusion in a built-in quasi-electric field
- Electron confinement
- Optical confinement
- Wide-gap window effect
- Diagonal tunneling through heterointerface.

Therefore, DHS structures open wide perspectives of various applications and results in diverse new classes of semiconductor devices:

- Low-threshold semiconductor lasers operating in cw mode at room temperature, lasers with distributed feedback (DFB) and distributed Bragg reflector (DBR) lasers, vertical surface-emitting lasers, IR type-II heterostructure lasers
- High effective LEDs
- Solar cells and photodetectors, based on the wide-gap window effect
- Semiconductor integrated optics, based on semiconductor DFB and DBR lasers
- Heterobipolar transistors (HBT) with wide-gap emitter
- Transistors, thyristors, dynistors with photon signal transmission
- High-power diodes and thyristors
- Infrared-to-visible converters
- Effective cold cathodes.

Fabrication of the new type of semiconductor structures and devices based on the heterostructures leads to new requirements for technology, for instance:

- Fundamental necessity for lattice-matched structures
- Multicomponent solid solutions used for lattice-matching
- Fundamental necessity for epitaxial growth technology.

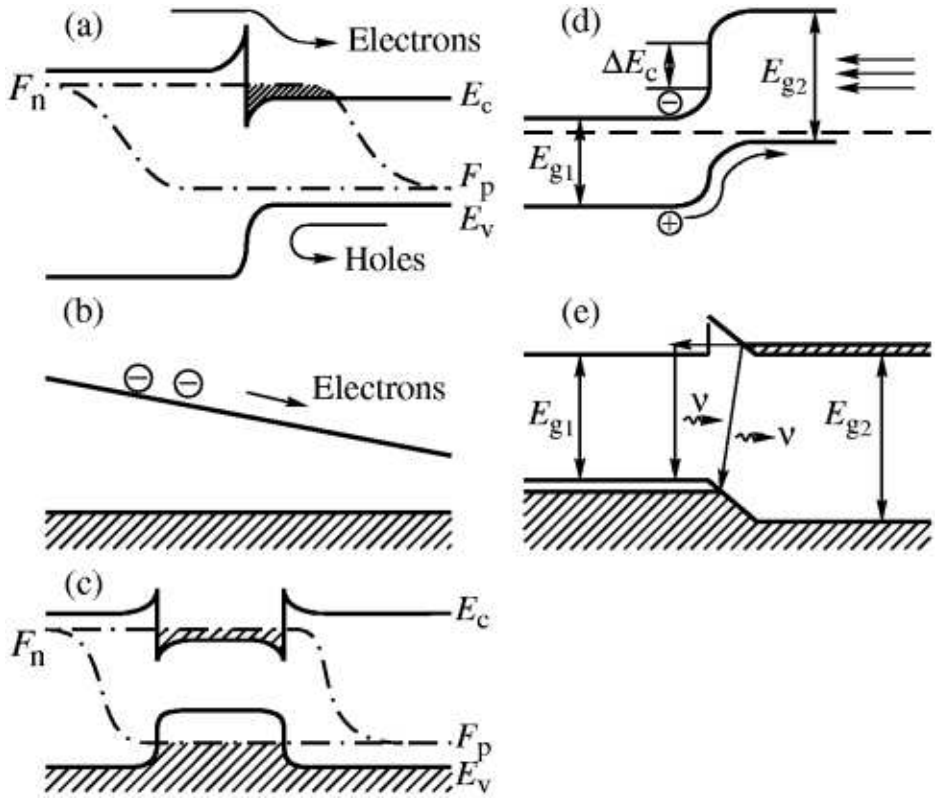

Fig 1. Fundamental physical phenomena in classical heterostructures: (a) one-side injection, (b) diffusion in built-in quasi-electric field, (c) electron and optical confinement, (d) wige-gap window effect, (e) diagonal tunneling across the heteroboundary.

In the early stage of the development of the heterostructure physics and technology, it became clear that new lattice-matched heterostructures are to be sought in order to cover wider spectral region. The first important step in this direction was made in the Laboratory of Physics of Semiconductor Devices in 1970; it was shown that various lattice-matched heterojunctions based on quaternary III–V solid solutions can be grown, which permitted varying independently the lattice constant and forbidden band gap [63]. Later, G. Antipas with co-workers came to the same conclusions [64]. As a practical example utilizing this idea were considered various InGaAsP compositions, and soon this material was recognized as the most important for a wide variety of practical applications: photocathodes [65] and especially lasers for fiber optical communications in the infrared [66,67] and visible spectral ranges [68–70].

After the first ideal classical heterostructures were created in the systems AlGaAs and InGaAsP the family of heterostructures grew very rapidly, and their present-day ("world map") is presented in Fig. 2.

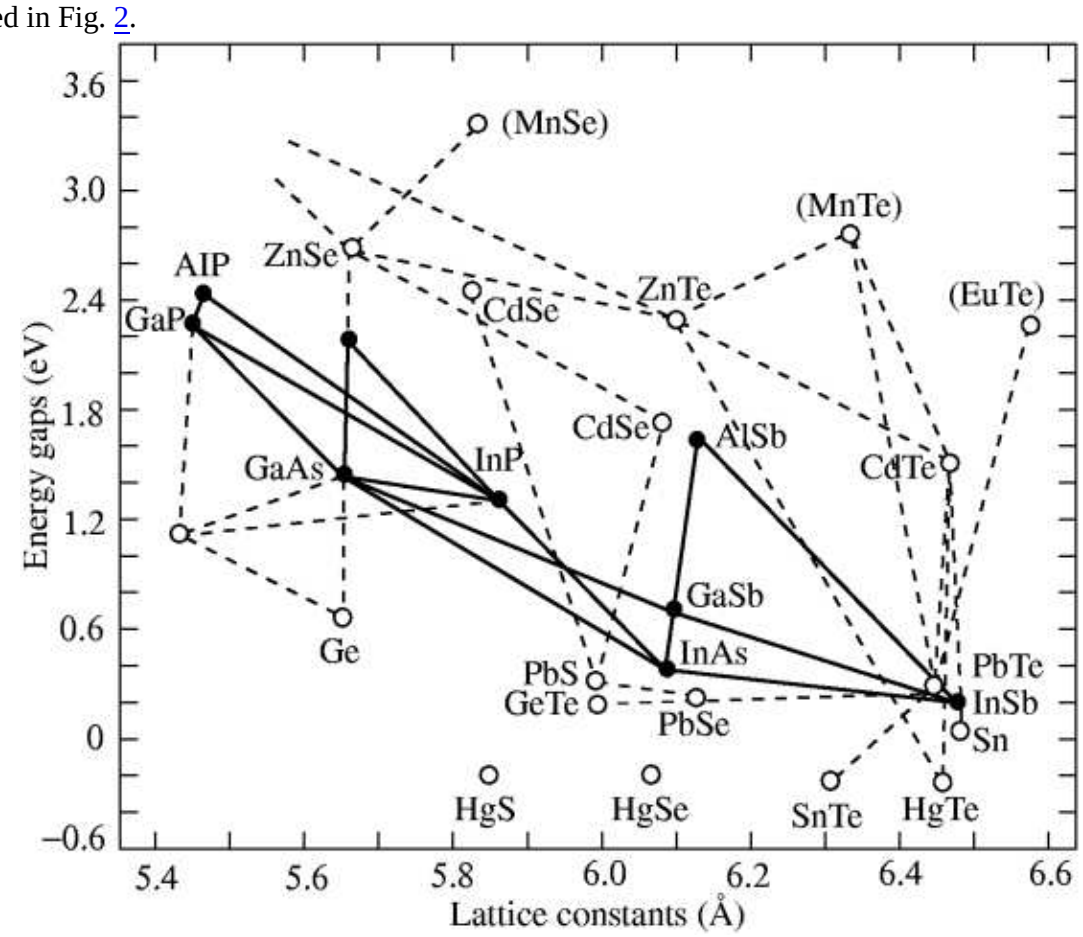

Fig 2. Dependence of the forbidden gap width on lattice parameter for Group-IV semiconductors and $A_{III}B_V$ and $A_{II}B_{VI}$ compounds. Investigated heterostructures are connected by lines (solid for $A_{III}B_V$, dashed for other compounds).

In the early 1980s, H. Kroemer and G. Griffits published a paper [71] which stimulated strong interest in staggered line-up heterostructures (type-II heterojunctions). Spatial separation of electrons and holes at interfaces of this kind ensures tunability of their optical properties [72,73]. Staggered band alignment furnishes an opportunity to obtain optical emission with a photon energy much lower than the forbidden band-gap width of each of the semiconductors forming a heterojunction. Fabrication of an injection laser based on type-II GaInAsSb-GaSb heterojunctions [73] opens up good prospects for creation of effective coherent light sources for the infrared. The emission in such a device is due to recombination of electrons and holes localized in self-consistent potential wells on different sides of the heterointerface. Thus, type-II heterostructures open up new possibilities both for development of the fundamental physics and for device applications which cannot be realized with type-I $A_{III}B_V$ heterostructures.

Quantum wells and superlattices

If the charge carrier motion in a solid is confined to a layer with a thickness of the order of the de Broglie wavelength of elementary excitations (or mean free path, which is shorter), then, in accordance with the quantum mechanics, quantum-size effects must be observed. In this case, a characteristic mass for quantization is the carrier (electron or hole) effective mass, rather than the free electron mass. Investigations of ultrathin layers became rather popular in the late 1950s–early 1960s (see, e.g., a review of V. Lutskii [74]). As objects of study were frequently used films of semimetals, e.g., bismuth, prepared by vacuum evaporation onto mica substrates. In thin Bi [75] and InSb films, the effective forbidden gap width increased with decreasing film thickness. In 1962, L. Keldysh studied theoretically the electron motion in a crystal in a periodic potential with a period much exceeding the lattice constant [76]. He predicted formation of minibands and occurrence of negative differential conductivity. In 1963, an idea was put forward [77,78] of using five-layer structures with two dielectric layers and an ultrathin intermediate layer to observe the effect of resonance tunnel current rise on crossing of the quantum-size level in the ultrathin layer by the Fermi level.

The material progress in fabricating quantum-size layers and investigating the quantum-size effects is associated with the development of the concept of semiconductor heterostructures and practical realization of ideal DHS. In 1969–1970, L. Esaki and R. Tsu proposed to use multilayer periodic semiconductor heterostructures with ultrathin layers (superlattices) for creating artificial materials with tunable miniband width [79]. A fundamentally important practical case of sequential tunneling in a superlattice was first considered at the Ioffe Institute by R. Kazarinov and R. Suris [80,81] in 1970. One of the first artificial superlattices of this kind was obtained at the Ioffe Institute by Zh. Alferov *et al.* in a multichamber VPE machine of special design in the system $GaP_{0.3}As_{0.7}$-GaAs also in 1970 [25]. In 1974, L. Chang *et al.* first observed the effect of resonant tunneling in MBE-grown ultrathin semiconductor heterostructures [82].

In 1970, R. Kazarinov and R. Suris considered at the Ioffe Institute the possibility of fabricating a unipolar long-wavelength laser operating on radiative electron transitions between quantum-size levels [80]. A laser operating on this principle was fabricated by F. Capasso *et al*. (so-called cascaded laser) only a quarter of century later [83].

In 1974, R. Dingle *et al*. experimentally confirmed for the first time the manifestation of the quantum-size effect in optical spectra of heterostructures with QWs [84]. A steplike character of the absorption spectrum, corresponding to the specific density of states in QWs, was demonstrated (Fig. 3). On making the QWs thinner, the steps are shifted to higher photon energies.

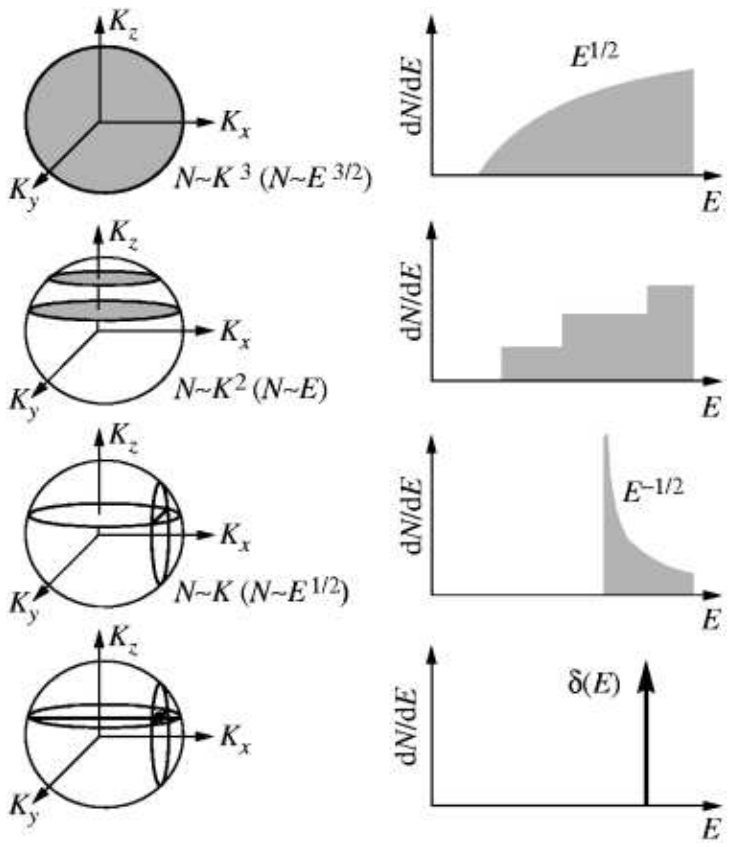

Fig 3. Density of states in structures of various dimensionality, calculated on the assumption that the carrier energy E in the band is a quadratic function of wave vector $\boldsymbol{k}$.

Beginning with the late 1970s and early 1980s, investigations of QWs and superlattices started to dominate in the physics of semiconductors. For example, the concept of modulation-doped heterostructures [85] made possible achieving unprecedented electron and hole mobilities, which enabled progress in studying the Quantum Hall Effect and predetermined the discovery of the Fractional Quantum Hall Effect [86].

Studies of the epitaxial growth of ultrathin layers of materials with varied lattice parameter demonstrated that in the initial stages the growth is pseudomorphic with no dislocation formatted, which made possible obtaining QWs and superlattices with elastically strained layers [87]—the so-called strained superlattices [88]. The use of strained superlattices enabled a significant broadening of the variety of materials usable for synthesizing perfect heterostructures.

By the end of 1980s, the main properties of QWs and superlattices were, on the whole, well understood and the interest of researchers progressively shifted toward structures with even lower dimensionality: QWRs and QDs.

Quantum wires and quantum dots

As follows from Fig. 3, dramatic increases in density of states (singularities) are observed at certain energies only in structures with QWRs and QDs. The limiting case of size-quantization occurs in QDs or, as they are also named, "superatoms." Semiconductor QDs in glassy matrices were proposed and realized by A. Ekimov and A. Onushchenko in 1980–1981 [89]. This work initiated important theoretical investigations of QDs started at the Ioffe Institute by Al. Efros and A. Efros [90]. The electron spectrum of an ideal QD is a set of discrete levels separated by forbidden regions, which corresponds to the electron spectrum of an isolated atom even though the real QD may consist of several hundred thousand atoms. Thus, there appears a unique possibility of modeling experiments of the atomic physics on macroscopic objects.

Methods of indirect fabrication of QWRs and QDs

During a long time attempts had been made all over the world to produce QWrs and QDs and devices based on them by "conventional methods," e.g., by selective etching of structures with QDs [91], local "intermixing" of structures with QDs by ion implantation or laser annealing, growth on profiled structures [92] and cleaved surfaces, and condensation in glass matrices [89]. However, the above methods of fabricating QDs and QWrs encountered serious difficulties. For example, with lithographic methods, the characteristic size of a resist molecule and/or metal mask grain (~ 10 nm) gives no way of obtaining reproducible QDs with controllable interface abruptness at the level of one and even several monolayers (ML) including also the cases when "dry" etching techniques (e.g., ion beam etching) are used. More fundamental problems are related to degradation of lateral surfaces during ion etching [91].

Spontaneous formation of ordered nanostructures

A breakthrough in fabricating ordered arrays of uniform QWRs and QDs became possible with the use of the effects of spontaneous appearance of periodically ordered structures on the semiconductor surface and in epitaxial semiconductor films.

Ordered nanostructures may appear in closed systems, e.g., on sample annealing or upon prolonged interruption of growth. Such structures are in equilibrium, and the thermodynamic approach is used for describing them. Ordered structures may also develop in open systems during crystal growth. In a broad sense the "self-organization" of nanostructures is understood as spontaneous development of a macroscopic order in an initially random distributions [93].

Spontaneously ordered nanostructure can be conventionally divided into four large classes:

(i) Structures with periodic composition modulation in epitaxial films of semiconductor solid solutions [94].

(ii) Periodically faceted surfaces [95,96].

(iii) Periodic structures of planar domains (e.g., islands of monolayer height) [97].

(iv) Ordered arrays of 3D coherently strained islands in heteroepitaxial lattice-mismatched systems [98].

In all of these systems, neighboring domains differ in lattice constant and/or surface structure and, consequently, domain boundaries are a source of long-range fields of elastic strain.

Both 2D and 3D islands can be used for obtaining QDs. In [99–101], buried InAs(001) layers in GaAs matrix obtained with submonolayer and monolayer depositions were studied by means of photoluminescence (PL). A conclusion was made that InAs forms microislands elongated in the [110] direction, all having the same width [100,101]. Later, the conclusion that islands of this kind exist in the system InAs/GaAs(001) in the case of a submonolayer deposition was confirmed by scanning tunneling microscopy [102] with the island width found to be 4 nm.

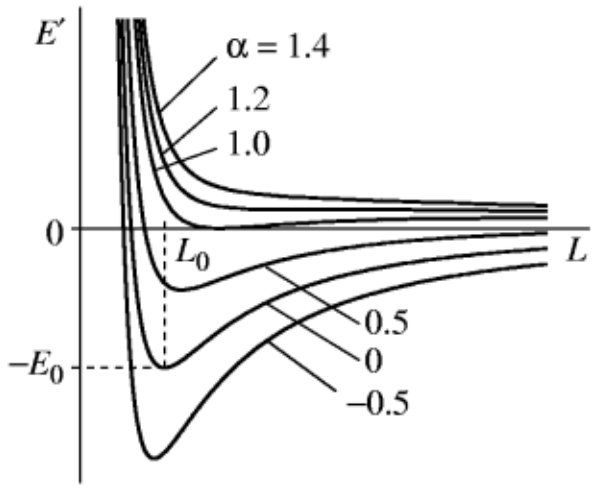

Fig 4. Energy of a sparse array of 3D coherently strained islands per unit surface area as a function of island size. The parameter α is the ratio between the change in the surface energy upon island formation and the contribution from island edges to the elastic relaxation energy. When $\alpha>1$, the system tends thermodynamically toward island coalescence. When $\alpha<1$, there exists an optimal island size and the system of islands is stable against coalescence.

Ordered arrays of 3D coherently strained islands. In lattice-matched heteroepitaxial systems the growth mode is determined solely by the relation between the energies of two surfaces and the interface energy. If the sum of the surface energy of epitaxial layer γ_2 and the energy of interface γ_{12} is lower than the substrate surface energy, $\gamma_2+\gamma_{12}<\gamma_1$, i.e., if the material 2 being deposited wets the substrate, then we have the Frank–van der Merve growth. Changing the $\gamma_2+\gamma_{12}$ value may result in a transition from the Frank–van der Merve mode to an Volmer–Weber one where 3D islands are formed on a bare substrate.

In a heteroepitaxial system with lattice mismatch between the material being deposited and the substrate, the growth may initially proceed in a layer-by-layer mode. However, a thicker layer has a higher elastic energy, and the elastic energy tends to be reduced via formation of isolated islands. In these islands the elastic strains relax and, correspondingly, the elastic energy decreases. This results in a Stranski–Krastanow growth mode.

Experimental studies of coherently strained islands arrays in the systems InAs/GaAs (001) and InGaAs/GaAs(001) have shown that a narrow size distribution of islands is possible [103,104]. The characteristic size is determined by the minimum in the energy of an array of 3D coherently strained islands per unit surface area as a function of the island size (Fig. 4) [98,105,106,107]. Interaction between islands via elastically strained substrate results in lateral island ordering typical of the square lattice.

Electronic structure and optical properties

Realization of ideal QDs. N. Ledentsov *et al.* demonstrated the formation of dense (~ 10^{11} cm^{-2}) arrays of dislocation-free InAs QDs in a GaAs matrix and studied the effect of growth parameters and QD composition on their optical properties [105]. The shape and size of QDs were determined for the first time, and lateral ordering of QDs into a square lattice with major axes aligned with the [001] and [010] directions was discovered. In the same work, cathodoluminescence spectra of QDs were studied with high spectral and lateral spatial resolution. It was shown that the PL line from the QD array broadened by fluctuations of shape and size in optical excitation decomposes into a set of ultranarrow lines from single QDs in the case of excitation by focused electron beam. It should be noted that the temperature-independence of the QD PL line width (contrary to two-dimensional and three-dimensional cases), first observed in [106] indicates unambiguously the atom-like nature of the electron spectrum of a QD (Fig. 5).

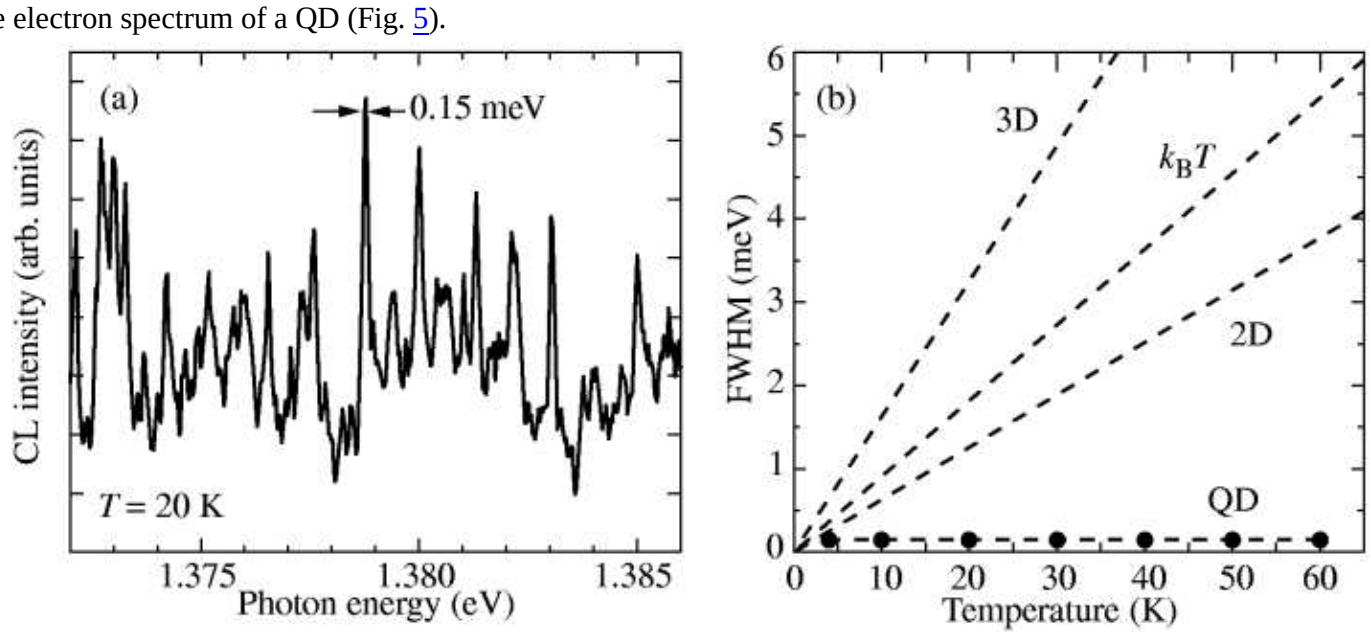

Fig 5. (a) Low-temperature (5 K) cathodoluminescence spectra taken with high spatial resolution from a structure with InAs QDs in a GaAs matrix and (b) temperature dependence of the linewidth for 3D, 2D, and isolated QD.

Absorption, photoluminescence, and luminescence excitation spectra for samples with QD arrays (Fig. 6) were also compared for the first time, and the unique features of optical properties for systems of this kind were determined [105]. For example, it was shown for the first time that the absorption peak of the ground state of a QD coincides with the PL peak for the same QD state. The authors noted that the resonant excitation of the QD ground state is only possible when the photon energy exactly corresponds to the atom-like spectrum of QD absorption. In a radiation recombination event, a QD emits a photon of exactly the same energy and, therefore, QD excitation and luminescence quanta can be generally separated in time-resolved experiments only. The given work also demonstrated for the first time that the QD excitation spectrum is modulated with an energy corresponding to the energy of LO-phonon in InAs, which is due to the fact that the

relaxation into the QD ground state is faster when the energy difference between the ground and excited states is a multiple of LO-phonon energy and, therefore, the possibility of radiationless recombination is lower in the excited state. Carrier capture by a QD directly from the matrix material occurs in times of order 1 ps. The time of relaxation from excited into ground state is not longer than 25–40 ps depending on the QD geometry [108]. In the case of resonant excitation [109,110] the PL spectrum decomposes into a series of lines. The energies of the observed peaks coincide with a multiple of GaAs- and InAs-related LO-phonon energies and combination of these including GaAs bulk phonons (36.6 meV), interface modes (34 meV), phonons of wetting InAs layer (29.5 meV), and InAs QD phonons (31.9 meV).

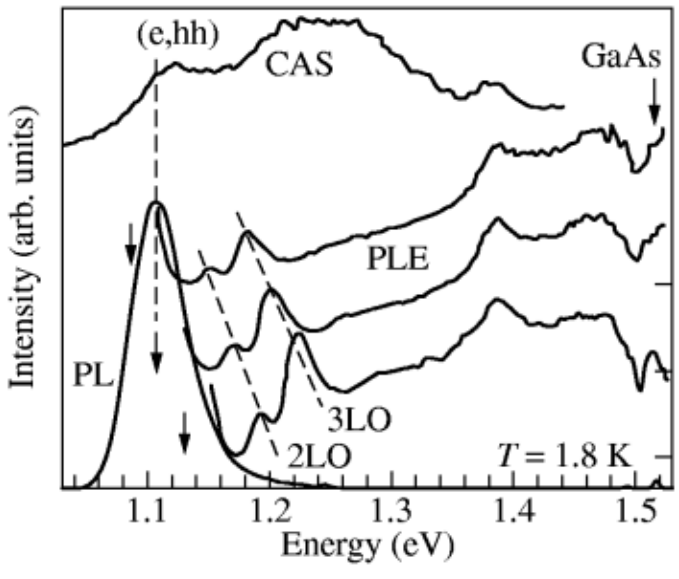

Fig 6. Spectra of calorimetric absorption, PL, and PL excitation for structures with QDs.

Relationship between growth modes and QD optical properties. The effect of growth interruption on the PL from InAs-GaAs structures with 3D QDs was studied in [109]. It was shown that increasing the number of deposited InAs up to 4 ML or making longer the interruption time in growth shifts the QD PL line to longer wavelengths (1.1 μm), which agrees with the increase in characteristic QD size observed by transmission electron microscopy (TEM). These results confirmed the existence of a "limiting" or "equilibrium" QD size indicated by TEM [109]. At low growth temperature (ca 350 $^{\circ}$C), QDs associate into elongated islands which is accompanied by the appearance of a peak at 1.8 μm (300 K) in PL spectra.

It was demonstrated that an array of ordered QDs exists only in a certain range of arsenic pressures [109].

Geometry of QDs. In the case of deposition at 460 $^{\circ}$C, pyramidal InAs QDs with square base (~ 120 Å) and major axes aligned with directions [001] and [010] and ~ 60 Å high are formed on the surface. Model calculations by molecular dynamics methods [111] indicate that an adequate cross-sectional image of a QD can be obtained by high-resolution TEM only under optimal defocusing conditions at a film thickness no more than doubled lateral QD size.

Luminescence from vertically coupled QDs. The luminescent properties of vertically correlated tunnel-coupled QDs were studied in [108, 112–114]. Increasing the number of QD deposition cycles resulted in a long-wavelength shift of both the PL line and the PL-resonant peak in the calorimetric absorption spectrum. Increasing the number of cycles makes shorter the radiative recombination lifetime in QDs. For large number of coupled QD lateral association of QDs in upper rows is observed together with the appearance of the corresponding long-wavelength PL peak.

Quantum dots of type-II. QDs of type-II were first studied by F. Hatami *et al*. in GaSb-GaAs [115]. In this system, holes are localized in the GaSb region, whereas for electrons these regions present a potential barrier.

Application of heterostructures in electronics

Semiconductor heterostructure lasers

Lasers based on classical heterostructures

Achieving a CW operation of semiconductor lasers at room temperature in 1970 was a historical event in the vigorous development of semiconductor heterostructure application.

In 1970, the international competition became exceedingly strong. Later, one of the major competitors, I. Hayashi, who worked with M. Panish at the Bell Telephone Co. Laboratory in Murray Hill, wrote [116]: "In September, 1969, Zhores Alferov of the Ioffe Institute in Leningrad visited our laboratory. We realized he was already getting a $J_{\rm th}^{(300)} = 4.3$ kA cm^{-2} with a DHS. We had not realized that the competition was so close and redoubled our efforts... Room temperature CW operation was reported in May 1970..."

In the paper of Zh. Alferov and co-workers submitted in May 1970 [117], CW lasing was realized in stripe-geometry lasers fabricated using photolithography and mounted on copper heat sinks coated with silver (Fig. 7). The lowest threshold current density $J_{\rm th}$ at 300 K was 940 A cm^{-2} for wide lasers and 2.7 kA cm^{-2} for stripe lasers. Independently, CW lasing in DHS lasers was reported by I. Hayashi and M. Panish [118] (for broad-area lasers with diamond heat sink) in a paper submitted only a month later than [117]. Achieving a CW lasing mode at room temperature caused an outbreak of interest in physics and technology of semiconductor heterostructures.

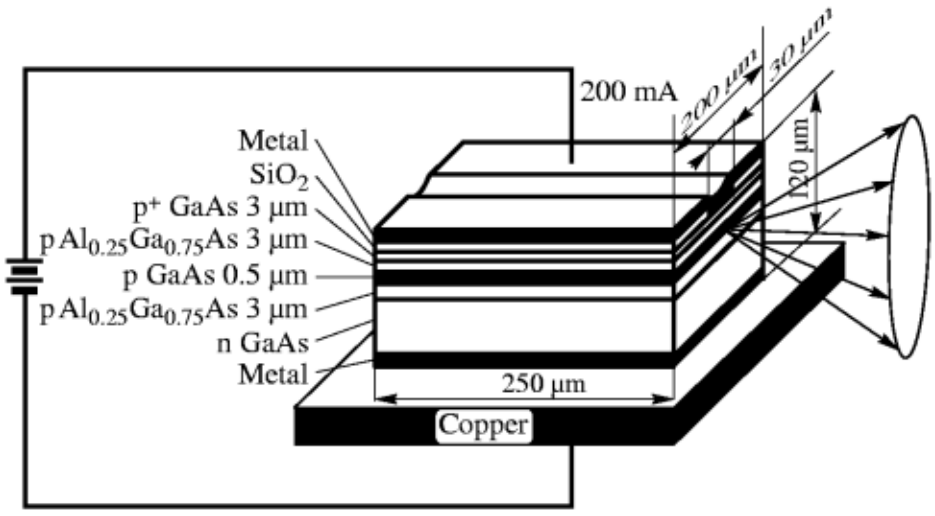

Fig 7. Schematic structure of the first DHS laser operating in CW mode at room temperature.

The basic concepts of a laser with distributed feedback (DFB) were formulated in Inventor's Certificate issued in 1971 [119]. In the same year H. Kogelnik and C. Shank considered the possibility of replacing the Fabri–Perot resonator or its like in dye lasers by periodic volume inhomogeneities [120]. It should be noted that their approach is inapplicable to semiconductor lasers, and all those who study DFB or DBR semiconductor lasers commonly use the approach formulated in [119]:

(1) Diffracting grating is created on the surface, rather than in the bulk of the waveguide layer.

(2) Interaction of waveguide modes with the surface diffraction grating not only gives rise to distributed feedback, but also produces well collimated output radiation.

A detailed analysis of the operation of a semiconductor laser with surface diffraction grating was performed in 1972 [121] where the possibility of single-mode generation was established. The first semiconductor lasers with surface diffraction grating and DFB were fabricated practically simultaneously at the Ioffe Institute [122,123], Caltech [124], and Xerox Lab in Palo Alto [125].

On the basis of semiconductor lasers with distributed Bragg reflector was obtained a practically temperature-independent lasing wavelength [126].

QW lasers

Lasing on QWs was first obtained by J. van der Ziel *et al*., but the generation parameters were much inferior to those of average DHS lasers [127]. Only in 1978, R. Dupuis, P. Dapkus in collaboration with N. Holonyak reported fabrication of a QW laser with parameters comparable with those of standard DHS lasers [128]. In this work, the term "quantum well" was first suggested. The actual advantage of QW lasers was demonstrated much later by W. Tsang from Bell Telephone. By significantly improving the MBE growth technology and designing an optimized structure (separate-confinement DHS lasers with graded-index waveguide: GRINSCH lasers), he could reduce the threshold current density to 160 kA cm^{-2} [129].

The development of MBE and MOCVD techniques for growth of $A_{III}B_V$ heterostructures was started at the Ioffe Institute in the late 1970s only. In the first place, it was stimulated the design and construction of the first Soviet MBE machine for domestic electronic industry. During several years, three generations of MBE machines were developed, the last of these named *Tsna* (a beautiful river not far from Ryazan', a city where the Research Technological Institute for Electronic Industry was situated: it is at this institute that the MBE machines were designed). In parallel and somewhat later, development of an MBE system was commenced at the Scientific and Engineering Association, Academy of Sciences, in Leningrad. In the late 1980s, several machines of this version were purchased by the Ioffe Institute. Both these types of MBE systems are still working at the Ioffe Institute and other laboratories of the country.

MOCVD systems were developed at the Ioffe Institute, and later, in the 1980s, a Swedish company Epiquip specially designed, with active participation of the researchers from the Ioffe two machines for the Institute.

A strong interest in low-dimensionality structures and the lack of equipment for MBE and MOCVD growth techniques had stimulated the investigations aimed at developing an LPE technique suitable for growing heterostructures with QWs.

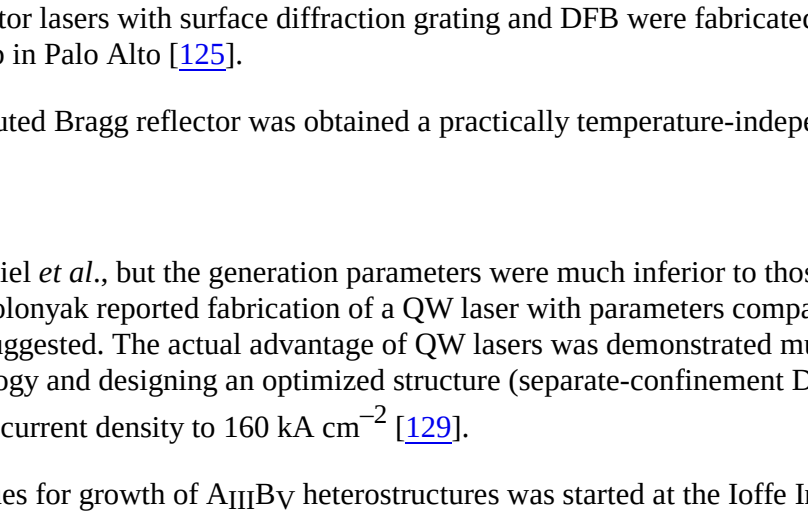

Fig 8. Watt–ampere characteristics of InGaAsP-GaAs SC DHS laser diodes with a single QW operating in CW mode. (1) Diode with weakly and strongly reflecting coatings, (2) diode with strongly reflecting coatings only. $N_E(I)$ is the dependence of energy conversion factor (efficiency) on current.

However, till the late 1970s, it seemed impossible to grow by LPE $A_{III}B_V$ heterostructures with an active region thinner than 500 Å, because of the existence near the heteroboundaries of extended transition regions of varying chemical composition.

The situation changed after the work of N. Holonyak *et al*. appeared. They proposed to use an LPE system with rotating "boats" for growing InGaAsP superlattices [130]. Zh. Alferov and co-workers developed a modified LPE technique with the usual translational motion of the substrate in a standard horizontal "boat" geometry for InGaAsP heterostructures [131] and a method of low-temperature LPE for AlGaAs heterostructures [132,133]. These techniques allowed to grow practically any type of high quality heterostructures with QWs with up to 20-Å thick active region and an interface region thickness comparable with the

crystal lattice parameter. Of great practical importance was the achievement with the use of the LPE technique of record-breaking threshold current densities in single-QW separate-confinement lasers based on InGaAsP/InP (λ = 1.3 and 1.55 μm) and InGaAsP/GaAs (λ = 0.65–0.9 μm) heterostructures [68].

In high-power stripe-geometry InGaAs/GaAs lasers (λ = 0.8 μm) (Fig. 8) it was achieved a 66% CW efficiency and 5-W radiation power at a stripe width of 100 μm and length of 1.2 mm [134,135]. These lasers were the first in which effective cooling of a power semiconductor device was effected by recombination radiation, as proposed previously in [20]. Another important feature of InGaAsP heterostructures was their rather high stability against development of dislocations and defects (Fig. 9) [136]. These studies laid foundation for wide use of Al-free heterostructures.

The most intricate laser structure with QWs combining a single QW and short-period superlattices (SPSLs) (Fig. 10) used for creating GRIN SCH (the most preferable for obtaining the lowest threshold currents) was fabricated at the Ioffe Institute in 1988 [137].

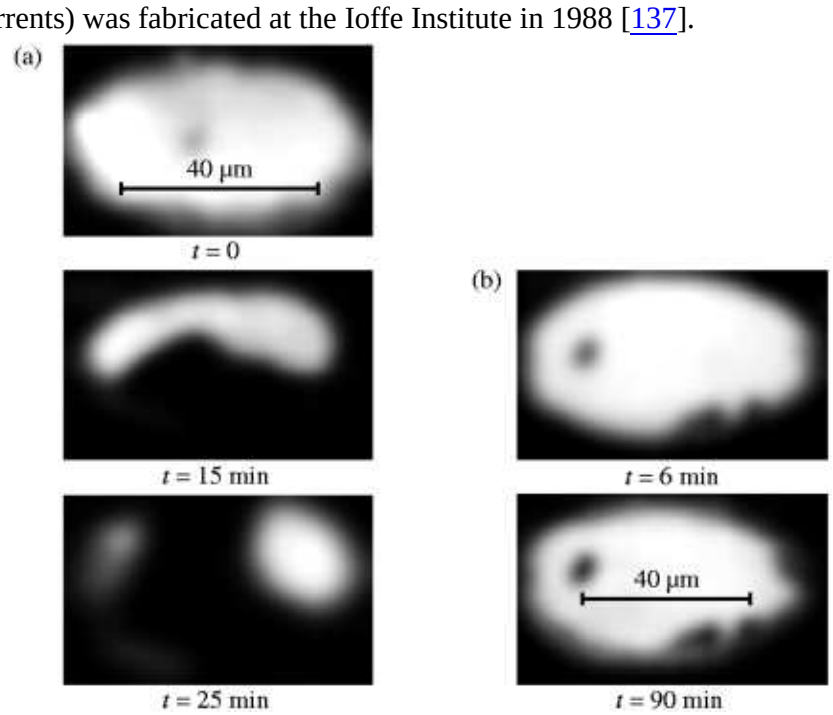

Fig 9. Temporal evolution of luminescence patterns from the active region in (a) AlGaAs-GaAs and (b) InGaAsP-GaAs SC DHS with a single QW at high excitation level. Kr^+ laser excitation beam diameter ~ 40 μm. Excitation levels, W cm^{-2}: (a) 10^4, (b) 10^5.

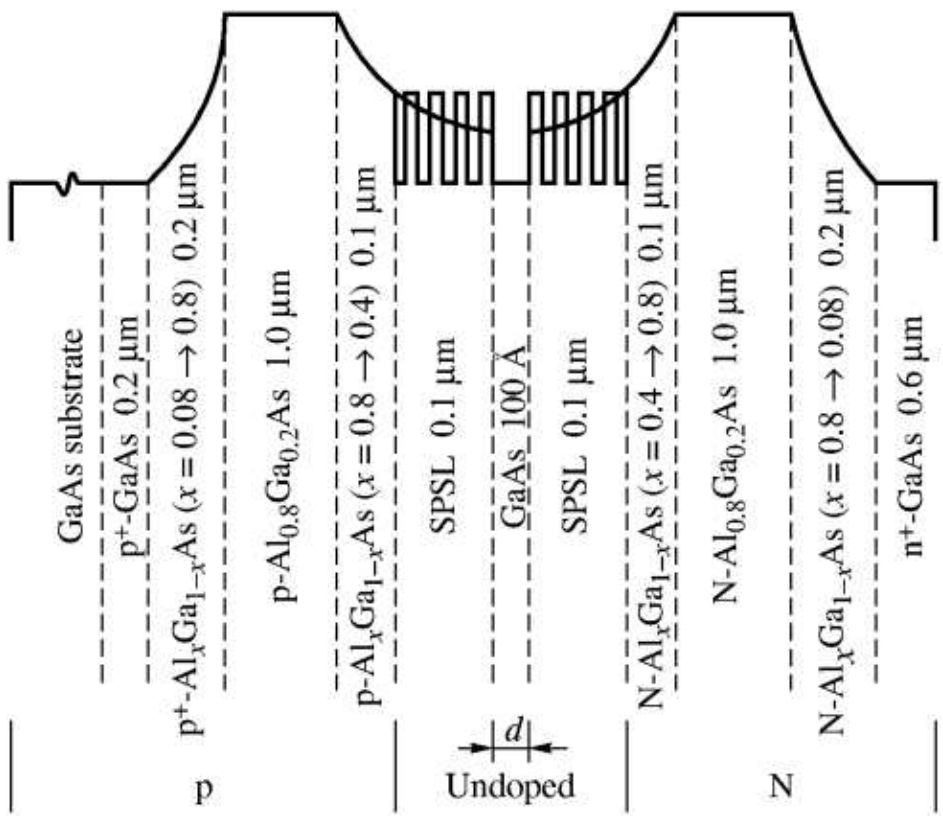

Fig 10. Structure of a SC DHS laser with QW confined by MBE-grown SPSL.

Use of SPSL not only gives a desirable profile of graded waveguide region and creates a barrier for defect propagation into the active region, but also improves the heterointerface smoothness and makes possible growing different parts of a structure at strongly differing temperatures. Thus, both a perfect surface morphology and a high internal quantum efficiency were simultaneously achieved on a planar GaAs (001) surface. Threshold current densities as low as J_{th} = 52 A cm^{-2} and, after certain optimization, even J_{th} = 40 A cm^{-2} were obtained which is still a world record for injection semiconductor lasers and serves as an excellent illustration of the effective use of QWs and superlattices in electronic devices.

The history of semiconductor laser development is, from a certain standpoint, the history of a struggle for reduction of their threshold current which is readily illustrated by Fig. 11. The most dramatic changes in this field occurred only after the concept of DHS lasers was implemented. The impact of SPSL QWs actually resulted in that the theoretical limit was achieved for this, most important parameter. Further opportunities are associated with the use of new structures with QWRs and QDs.

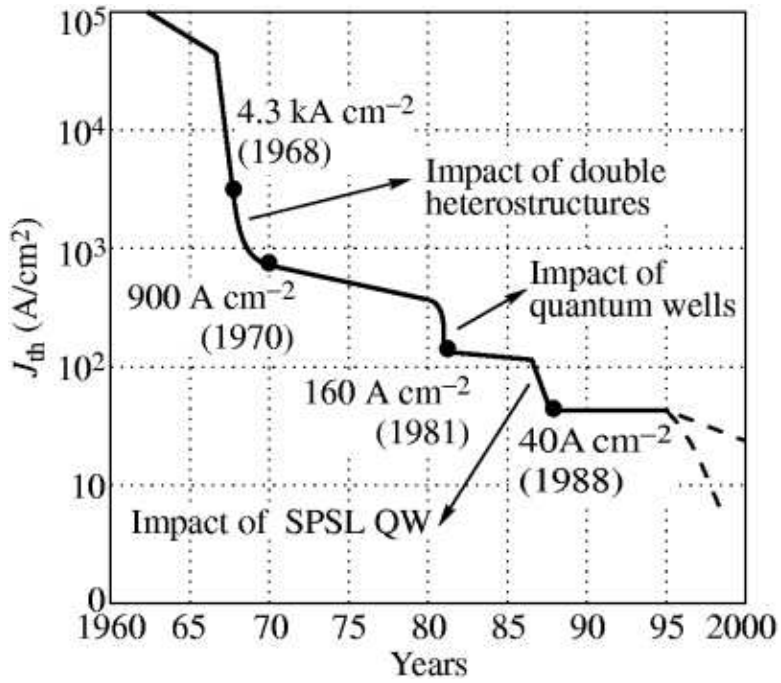

Fig 11. Evolution of the threshold current of semiconductor lasers.

QWR and QD lasers

QWR lasers. Significant advantages of QWR and QD lasers over QW devices were predicted in [138]. Historically, injection QWR lasers were first obtained by growing structures in V-grooves [139]. The energy difference between size-quantization subbands in such QWRs is comparable with kT at room temperature, in-plane quantum-size effects are difficult to observe, and no significant difference between this laser and QW laser was revealed.

QD lasers. Lasing under optical excitation via states of self-organized QD was first observed in 1993 [140]. Soon after, the first injection laser containing a single sheet of InGaAs QDs in the active region was fabricated [141]. At low temperature lasing started at energies close to the QD PL peak indicating that transitions via the ground states of QDs are responsible for lasing. With increasing temperature, the threshold current density remained practically unchanged retaining its value of 80 kA cm^{-2} to temperatures of about 180 K. With the temperature dependence of the threshold current density approximated by $J = J_0\exp(-T/T_0)$, $T_0 = 380$ K in this temperature interval which is higher than the theoretical limit for QW lasers.

The material gain was determined directly from the condition that gain is equal to loss at the lasing threshold [113,142]. The experimental value of the maximum "specific gain" was 1.5×10^5 cm^{-1} [142], which is two orders of magnitude higher than in the case of QW lasers. The differential gain of QD lasers at the lasing threshold is also markedly higher than in QW lasers being equal to ~ 10^{-12} cm^2.

The modal gain can be enhanced by increasing the QD concentration which is achieved by using vertically correlated QDs [108, 112–114]. With these lasers the possibility of generation via the ground state of QDs up to room temperature was demonstrated [112]. It was also shown that the threshold current density decreases dramatically to ~ 90 kA cm^{-2} (300 K) on increasing the number of stacking cycles to 10 [108,113,114].

The threshold current density in lasers was further reduced by using AlGaAs instead of GaAs as a matrix for vertically correlated QDs [108,114] which allowed reducing the threshold current density at room temperature to 60 A cm^{-2} [108] and increasing the differential efficiency to more than 70%. Thus, it was realized a CW mode of operation of a QD laser at room temperature with an output of 1.5 W and more. The generation went via QD states up to pumping currents exceeding 10–20-fold the threshold values, and the efficiency of the device in CW mode was as high as 42%.

Dynamic properties of QD lasers. The good dynamic characteristics of the QD laser were determined by the high differential gain coefficients [142]. Direct measurements of the cutoff frequency of a QD laser gave a value of the order of 10 GHz [143]. The experimental values of the lasing line spectral broadening factor (α-factor) were ~ 0.5, which was much lower than in the case of QW laser.

Theory of QD lasers.
First detailed descriptions of a realistic QD laser with a strong nonuniform gain line broadening were given by L. Asryan and R. Suris at the Ioffe Institute [144,145] and M. Grundmann and D. Bimberg at the Technical University in Berlin [146,147] who showed that even with account of a substantial nonuniformity of QDs (10% size scatter) such lasers must essentially outperform QW lasers.

Surface-emitting QD lasers. Injection lasers based on vertically stacked isolated QDs were fabricated by H. Saito *et al*. The threshold current density at room temperature was 5000 A cm^{-2} [148], with lasing via excited QD states. To improve the working parameters of vertical QD lasers, the concept of vertically correlated QDs as active medium was proposed [149]. In structures with a 10-μm aperture it was realized a CW lasing mode at room temperature with a threshold current of 180 μA (180 A cm^{-2}, 300 K). The maximum efficiency was 16%. The minimum threshold current was 68 μA for 1-μm mesa-structure, which corresponds to the best values for vertical lasers based on QWs of similar geometry.

Exciton waveguides.
Realization of the waveguide effect assumes the presence of a thick (with thickness comparable to the wavelength in the crystal) layer with high average refractive index. N. Ledentsov and co-workers proposed a concept of "exciton waveguide effect" in a laser in which the waveguide effect is achieved through resonant modulation of the refractive index, related to resonant exciton absorption in a structure with QDs ("submonolayer" superlattice) [150]. Lifting of the selection rules for momentum and the absence of the exciton screening effect in QDs results in that the lasing is of phononless nature. The resonant waveguide effect is realized now both in $A_{II}B_{VI}$ [150] and in $A_{III}B_{V}$ systems.

Self-adjusted microcavities.

Since the material gain of QDs is rather high and there is no screening of exciton states in QDs, the modulation of the refractive index due to Kramers–Kronig relations, can automatically tune the vertical laser resonator mode within the gain line contour. A similar effect was observed in studying the interaction of the line of exciton absorption in a QW in the cavity mode with a pronounced spectral splitting (7 nm) of the transmission line observed [151]. However, screening of excitons at high excitation densities gives no way of realizing this effect in vertical QW lasers, and the gain lines and the resonator mode are not interrelated [152]. In [149], the effect of annealing on the properties of vertical lasers with InGaAs-GaAs QDs was studied. Annealing of QDs shifted the maximum gain to shorter wavelengths with the lasing wavelength also shifted by 6 nm (this is not characteristic of QW structures); the occurrence of the effect of self-adjustment of the resonator mode and the gain band of the vertical QD laser was demonstrated for the first time.

Infrared QD emitters.
The time of phonon relaxation in a QD in transition from excited to ground state can be made much longer (up to 40 ps in the case of comparatively large QDs) as compared with the QW case where the time of subband relaxation is only ~ 1 ps. This fact and the lack of lateral transport of nonequlibrium carriers in QDs are the reasons for a higher probability of interlevel carrier relaxation in QDs by emitting far infrared quanta. L. Vorob'ev *et al*. observed for the first time IR emission (10–20 μm) from QD lasers operating in the near-infrared range [153].

Prospects for development of emitters with InAs QDs in silicon. The idea of using InAs QDs in silicon matrix for fabricating high-efficiency silicon-based light-emitting devices is of much interest. Recent fabrication of 3D InAs islands in Si matrix [154] and demonstration a line of PL from silicon-overgrown InAs QDs (1.3 μm at 77 K and 1.6 μm at 300 K)indicate that this direction shows great promise.

Heterostructure light-emitting diodes

Heterostructures have a number of advantages over homo-p-n-junctions, as regards LED parameters. When the active region is made of a material with a narrower gap than that of the material through which radiation is emitted, loss of light in passive regions of the structure is reduced, and the unidirectional type of injection in heterojunctions lowers loss by carrier recombination in emitters. These advantages were first actualized in AlGaAs heterostructure LEDs in which, owing to the absence of any additional surface states at the heteroboundary, a nearly 100% internal quantum efficiency of radiative recombination was achieved [155,156].

The effect of re-emission consisting in multiple absorption of generated light with the subsequent radiative recombination of electron-hole pairs excited by light was discovered and studied (Fig. 12) [157].

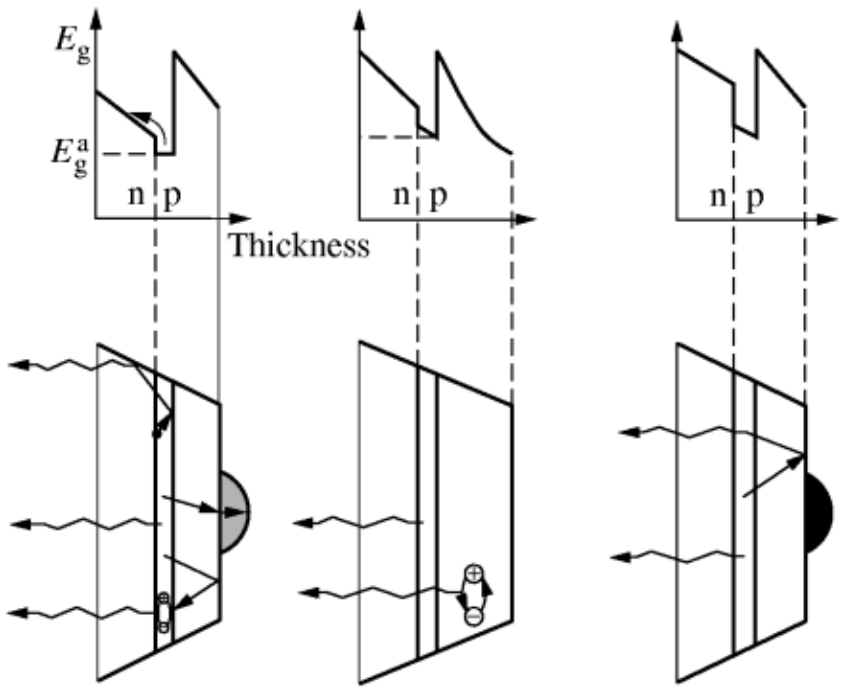

Fig 12. Forbidden gap width in AlGaAs/GaAs heterostructure LEDs of three types and schematic of light reflection and "re-emission" processes.

The results obtained were used to develop high-efficiency sources of spontaneous radiation on structures with a layer of a narrow-gap semiconductor sandwiched between two wide-gap layers, in which the effects of multiple reflection and re-emission of light in the active layer were used and loss of light by absorption in passive regions of the structure was reduced [47][158,159,160]. These structures yielded record-breaking values of external quantum efficiency: in LEDs with semi-spherical antireflection coatings η_e = 45% at $h\nu$ = 1.4–1.5 eV, 20% at $h\nu$ = 1.75 eV, and 5–10% at $h\nu$ = 1.8–1.87 eV.

Long-wavelength GaInAsSb/GaSb heterostructure LEDs (λ = 1.7–2.5 μ m). The 2-μm spectral region including the water absorption line (λ = 1.94 μm) used in optical monitoring and absorption lines of methane CH_4 at 2.32–2.35 μm is of particular interest for LED designers.

The spontaneous light emitter developed at the Ioffe Institute for this spectral region [161,162] was a semiconductor structure comprising an active n-GaInAsSb layer sandwiched between an n-GaSb substrate and a wide-gap p-GaAlAsSb emitter (E_g~ 1.2 eV). Room temperature emission spectra of the LEDs show a single band whose peak wavelength practically linearly depends on the composition of the solid solution in the active region. The external quantum efficiency of the LEDs is the highest (η = 4%) at 2.0–2.2 μm.

Uncooled long wavelength non-isoperiodic InAsSb/InAsSbP heterostructure LEDs (λ = 3–6 μm).
The requirements to air purity in industrial areas becoming more and more stringent, efforts of quite a number of researchers are aimed at developing photon-coupled pairs "LED-photodetector" operating in the mid-infrared spectral range (3–6 μm) and sensitive to major air contaminants, such as C_nH_m, SO_2, NH_3, CO_2, CO, etc., whose absorption lines lie in this spectral range.

LEDs for the 3–6 μm spectral range were developed using heterostructures based on InAsSb narrow-gap solid solutions [163,164]. One of the main difficulties in developing long-wavelength LEDs consists in the lack of an isoperiodic substrate for InAsSb solid solutions, which predetermines the use of strained non-isoperiodic heterostructures in the system InAs/InAsSb/InAsSbP for creating long-wavelength LEDs. Figure 13(a) shows a double InAsSb/InAsSbP heterostructure grown on an InAs substrate [163]. Emission spectra of the LEDs (λ = 3–4 μm) are shown in Fig. 13(c).

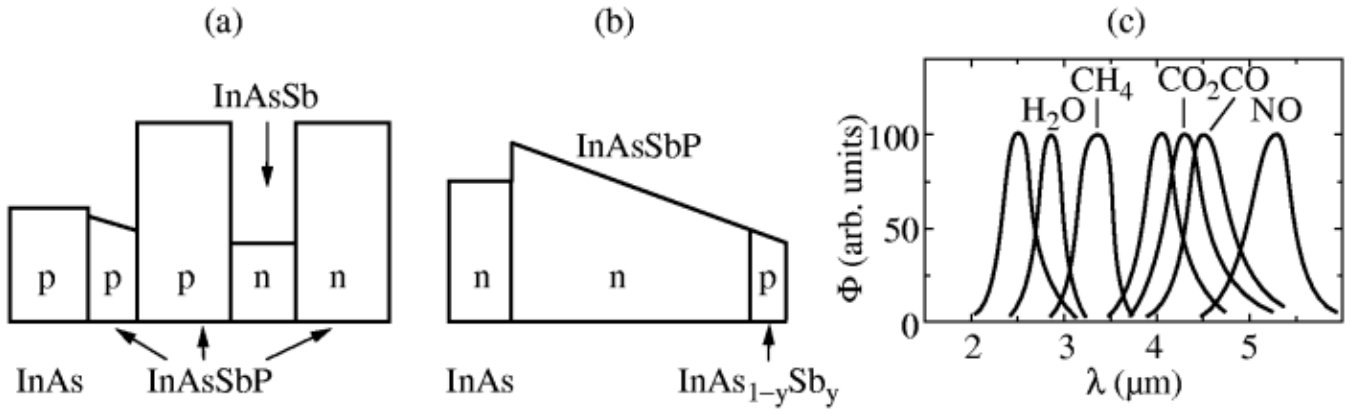

Fig 13. Band diagrams for (a) heterostructure LED (λ = 3–4 μm), (b) graded bandgap LED (λ = 4–6 μm), and (c) emission spectra for long-wavelength LEDs.

With the use of gradient structures, structurally perfect InAsSbP (Fig. 13(b)) and InGaAs layers and uncooled LEDs with λ>4 μm were fabricated for the first time. These LEDs have found use in devices measuring the content of carbon mono- and dioxide. Spectra of LEDs of this kind are also shown in Fig. 13(c).

Recently, effort has been made to extend the operating range of InAsSb LEDs to longer wavelengths. Efficient LEDs were developed, emitting light with λ = 5–6 μm (300 K). These LEDs have the narrowest, among spontaneous emitters, emission band (<0.6 μm), which makes them suitable for creating a new generation of nitrogen oxide (NO) sensors with an operating wavelength λ_{max} = 5.3 μm.

Heterostructure solar cells and photodetectors

Solar cells

$A_{III}B_V$ heterostructure solar cells can be used to produce solar batteries with higher efficiency and radiation hardness. An important advantage of heterostructure photoelectric converters is their ability to efficiently convert strongly concentrated (up to 1000–2000-fold) sunlight, which opens up possibilities of reducing significantly (in proportion to the extent of concentration) the area and cost of solar cells and, as a result, making cheaper the "solar" electric power.

n-GaAs–p-AlGaAs heterostructure solar cells were first proposed and fabricated at the Ioffe Institute [165]. The use of a wide-gap "window" made of a thin layer of an AlGaAs solid solution (Fig. 14(a)), which is practically fully transparent for the sunlight, ensures passivation of the surface of the photoactive region [166,167] and gives efficiencies close to the limiting theoretical values [168]: 24.6% for 100 suns in space and 27.5–28% for 100–200 suns in Earth conditions.

In recent years MOCVD has been widely used for fabricating AlGaAs/GaAs heterostructures for solar cells. Of particular interest is a MOCVD-grown heterostructure solar cell with a built-in Bragg mirror. In a structure developed at the Ioffe [169], the backside potential barrier is replaced with a multilayer dielectric mirror comprising 24 alternating GaAs (60 nm) and AlAs (70 nm) layers. The reflectivity of such a mirror is about 95% in the spectral range 750–900 nm. As a result, that part of solar radiation which is not absorbed in the base layer is reflected into the active region (Fig. 14(d)), so that the collection efficiency for carriers generated by light remains high at thinner base region and shorter diffusion lengths, which increases the radiation hardness of solar cells [169].

Owing to their higher efficiency and improved radiation hardness, AlGaAs/GaAs heterostructure solar cells are widely used in space. In the solar battery of the command module of *Mir* space-station were installed heterostructure solar cells with a total area of 60 m^2 fabricated by the technique developed at the Ioffe Institute and operating until now.

The efficiency can be increased further by using cascade solar cells [170–174] comprising multilayer heterostructures with two or more p-n junctions in materials with different gap widths (Fig. 15). In such elements the "top" p-n junction formed in a wider-gap material is intended for efficient conversion of the short-wavelength part of the solar spectrum, and the "bottom" p-n junction made of a narrower-gap material is optimized for conversion of the long-wave radiation passing through the wide-gap cell.

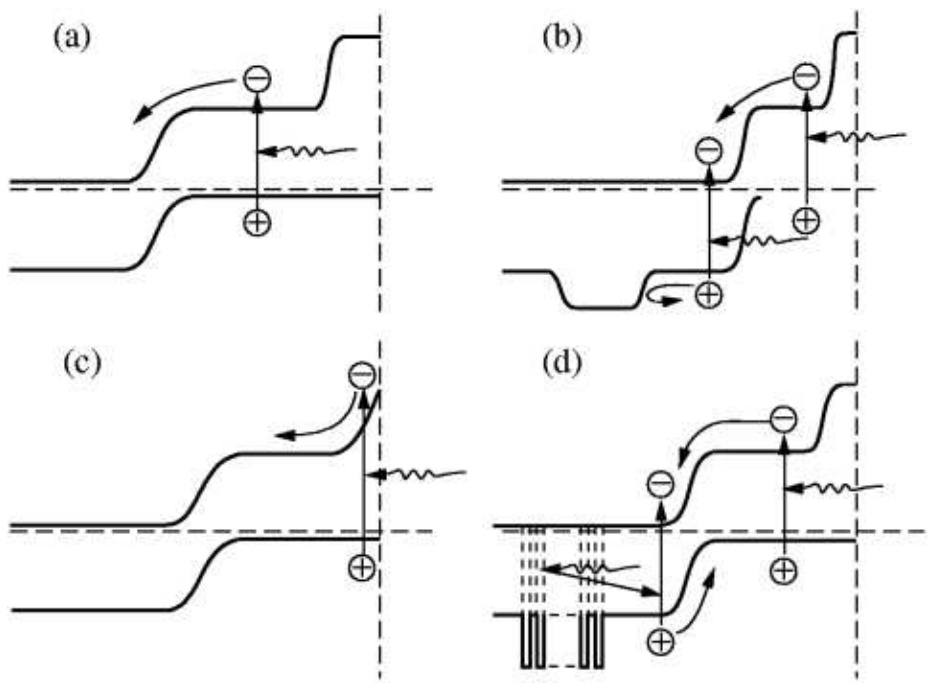

Fig 14. Band diagrams for AlGaAs/GaAs heterostructure solar cells: (a) structure with p-n junction in GaAs and frontal wide-gap p-AlGaAs "window;" (b) structure with backside potential barrier in n-region; (c) structure with an AlGaAs frontal layer of varied composition; (d) structure with a Bragg "mirror" in n-region.

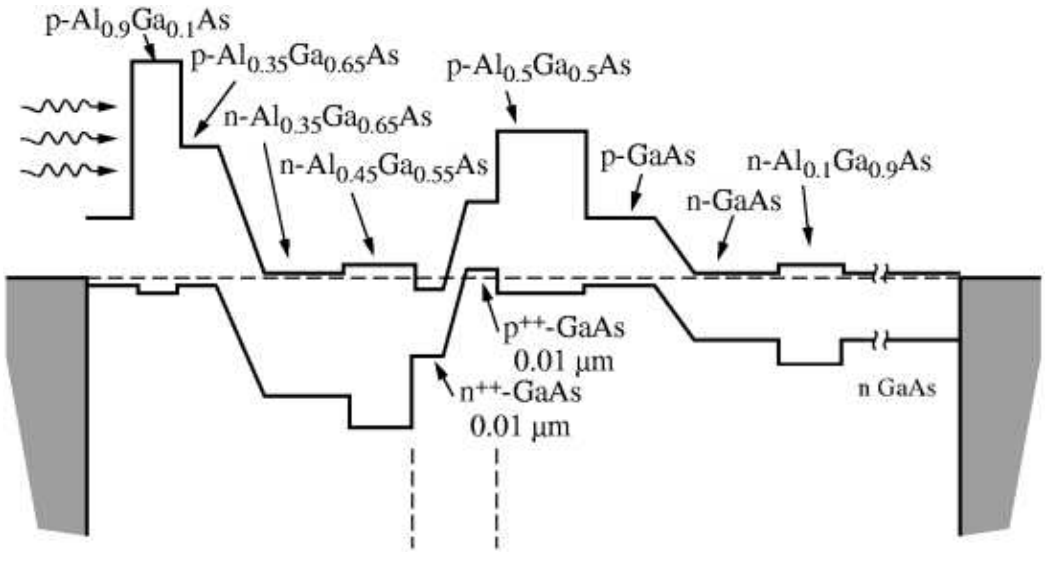

Fig 15. Band diagram for a monolithic cascade solar cell with AlGaAs/GaAs heterojunctions, fabricated by low-temperature LPE.

The increase of efficiency in cascade cells was demonstrated at the Ioffe Institute on a mechanically stacked cell [171]. In this design, GaAs is used as a material for the wide-gap cell and GaSb or InGaAs as a material for the narrow-gap one. The GaAs cell is made transparent for infrared radiation with wavelength exceeding 0.9 μm, and the narrow-gap cell ensures efficient conversion of the long-wavelength part of solar radiation in the spectral range 0.9–1.8 μm. The efficiency of such solar cells is 32–33% for AM1.5, 50–100 suns.

Of considerable interest is a monolithic cascade solar cell (Fig. 15) in which the "top" and "bottom" cells are connected by a tunnel p^+-n^+ junction providing for low ohmic loss. Cascade cells of this kind were fabricated using AlGaInP/GaAs [172,173] and AlGaAs/GaAs [174] heterojunctions. The highest efficiencies achieved in these elements are 30–31% [172,173] for direct and concentrated AM1.5 sunlight.

Photodetectors

Heterostructures based on $A_{III}B_V$
materials and their solid solutions are widely used now in new types of photodetectors: GaAs/AlGaAs-based for the spectral region 0.3–0.9 μm, InP/InGaAsP-based for the 1.0-1.6 μm range, and the GaInSbAs system for longer wavelengths (2.0–6.0 μm). Nearly all these heterostructures were first fabricated at the Ioffe Institute. It was shown that the use of heterojunctions in photodetectors not only does enable control over their spectral sensitivity region, but also makes it possible to increase the quantum efficiency and speed of photodetectors by bringing into coincidence the regions of light absorption and separation of nonequilibrium carriers, to reduce dark currents, and, in some cases, to control impact ionization processes [37,175]. AlGaAs-GaAs heterostructures were used at the Ioffe Institute to fabricate first fast heterophototransistors with low dark current, high-efficiency vertical isotype N-n^0-n^+ heterostructure photoresistors, and vertical field effect phototransistors with a response time of ~10^{-10} s [175,176].

InGaAsP/InP heterostructure photodetectors. In the early 1980s, in connection with the development of a glass fiber with low loss at 1.3–1.55 μm, intensive work was commenced all over the world on creating photodetectors for this spectral region based on InGaAsP solid solutions. To create fast and low-noise high-performance light-sensitive devices, such as p-i-n photodiodes and avalanche photodiodes, phototransistors, and photoresistors, the problem was to be solved of preparing high-purity (n<10^{16} cm^{-3}) epitaxial InP and InGaAsP layers [177]. A simple method for growing high-purity layers by the LPE technique was proposed and developed at the Ioffe Institute. The method consisted in doping growth solutions with isovalent rare-earths, such as Y, Nd, Gd, Td, Dy, Er, Ho, and Yb. The resulting InGaAs/InP p-i-n photodiodes had a sensitivity S_λ = 0.5–0.7 A W^{-1} in the spectral region 1.3–1.55 μm [178] at a response time of ≤ 50 ns.

Photodetectors for the spectral region 2–5 μm. As was mentioned above, spectral region 2–5 μm is important for express ecological monitoring and gas analysis.

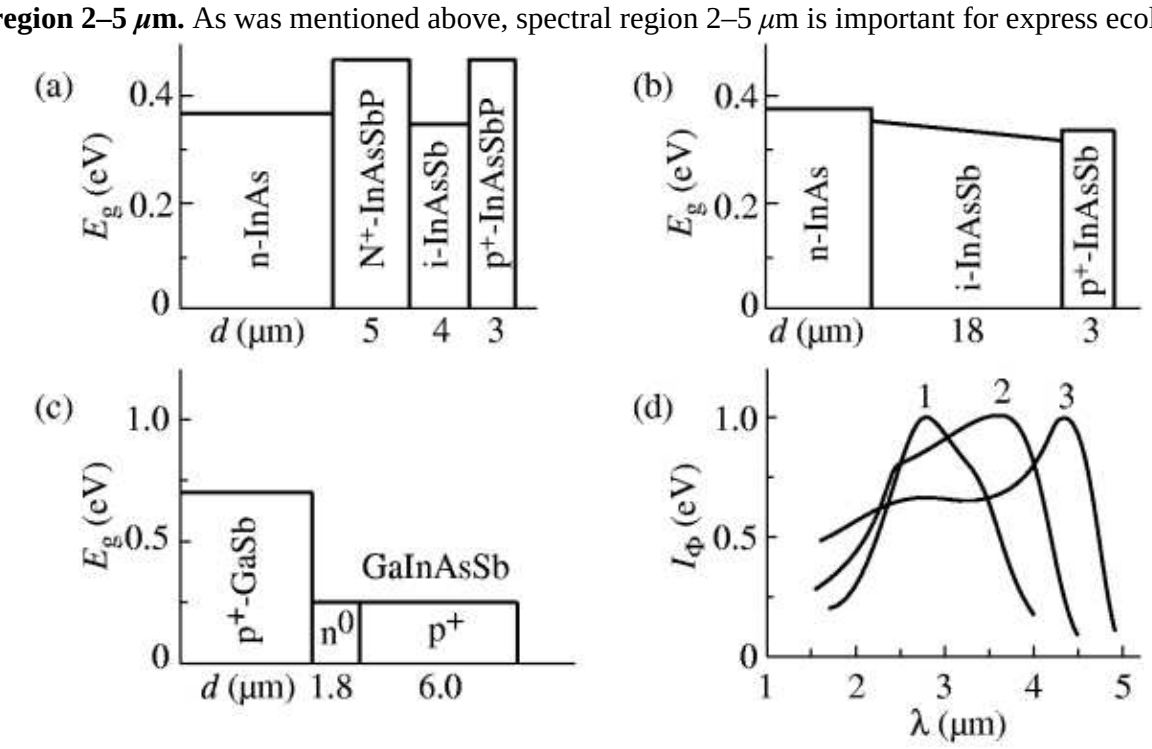

Fig 16. (a)–(c) Schematic of photodiode heterostructures and (d) spectral characteristics for indicated photodiodes at room temperature: curve 1 for (a), curve 2 for (b), and curve 3 for (c).

Uncooled GaInAsSb/GaAlAsSb photodiodes with a quantum efficiency of
~ 0.9–1.0 A W^{-1} and response time of ~ 0.5 ns operating in the spectral range 1.2–2.4 μm and also fast p-i-n heterophotodiodes having lightly doped GaInAsSb active layer, which enabled achieving as short a photoresponse time as 100–200 ps, were first fabricated at the Ioffe Institute by LPE onto GaSb substrates [179]. For the first time, uncooled and slightly cooled long-wavelength InAs/InAsSbP, InAsSb/InAs, and GaSb/InGaAsSb heterostructure photodiodes were developed (Fig. 16) for the spectral range 3–5 μm [180,181] with quantum efficiency of 1.2 A W^{-1} at a wavelength λ = 3 μm and response time of ~ 50 ns. Also for the first time was discovered the phenomenon of "resonance" impact ionization in GaSb and InAs-like materials in which the forbidden gap width is close to the valence band spin-orbit splitting [182]. As a result, long-wavelength avalanche photodiodes with low level of excess noise were created on the basis of materials with high

ratio of impact ionization coefficients for holes and electrons (≥ 20–60). Fast avalanche photodiodes of this kind for the spectral range 2–4 μm were developed using InAs, InAsSb, and GaAlAsSb/GaSb [182], and also GaInAsSb/GaAlAsSb heterostructures with separated regions of multiplication and absorption [183].

Devices for superhigh-speed electronics

Pulsed semiconductor devices.
In the middle 1970s, an LPE technique for preparing undoped epitaxial GaAs layers and fabricating on their basis high-voltage p-n junctions with a breakdown voltage as high as 1.8 kV was developed at the Ioffe Institute. A strong modulation of the resistance of the high-resistivity base region by the intrinsic recombination radiation was revealed and means were found of enhancing this effect [184]. The development of a technique for growth of undoped epitaxial GaAs layers enabled proceeding to fabrication of more intricate structures—pulsed thyristors and transistors.

The high internal quantum efficiency of radiative recombination and the possibility of controlling in the course of epitaxial growth the forbidden gap widths of layers constituting the p-n-p-n structure made it possible to propose and study thyristors in which the turn-on voltage was controlled by intermediate conversion of the electric control signal into an optical one with the subsequent reverse conversion into an electric signal at the collector junction [185,186,187].

A significant increase in the turn-on voltage (to 1.5 kV) and speed was achieved in structures named photon-injection switches (PIS) [188]. A schematic of a PIS structure is given in Fig. 17. A characteristic feature of this structure is that, depending on the connection type, PIS can operate both as a fast pulsed thyristor and as a transistor. In the developed devices, comparatively slow diffusion-drift processes of nonequilibrium carrier transport in base regions were replaced by practically inertialess photon transport, which increased by more than an order of magnitude of the operating speed. In a PIS operating in the thyristor mode, the time of anode current rise is not longer than 100 ps, and the switching is stable to within 10–15 ps [187,189]. In a structure connected as a transistor, the role of the base current is played by the photon flux from the LED part absorbed in the collector region of the n-n-p-n^+ transistor operating as a phototransistor. Despite the multistage nature of the conversion, the amplification coefficient in a circuit with common base is as high as 20–50. By now, transistors have been developed with collector-emitter voltage capacity of 500 V, pulse currents of up to 20 A at β = 10, and signal rise and decay times of ~ 10 ns.

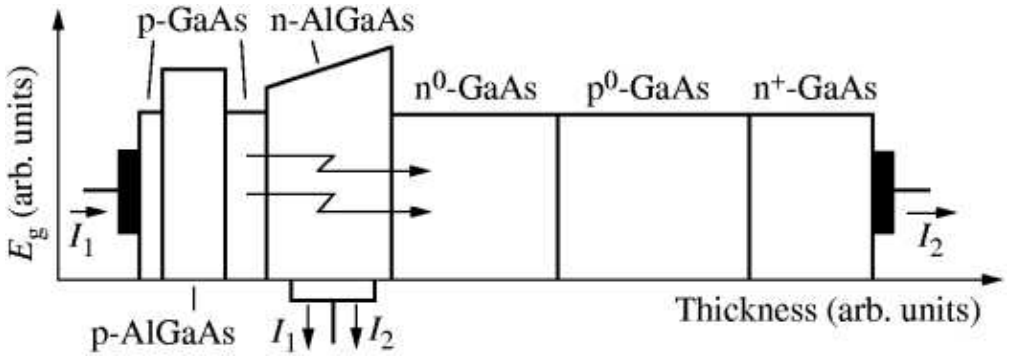

Fig 17. Forbidden gap profile along the structure of a photon-injection switch. Currents are shown for transistor connection: I_1—control current, I_2—output current. In thyristor connection, the current I_2 flows through the whole structure.

Heterobipolar transistors.
As already noted, practical interest in heterojunctions arose in 1951, when, to increase the efficiency of the emitter junction at high injection levels, W. Shockley proposed a transistor with emitter having wider-gap emitter than the base region. However, only after a technique for fabrication of GaAs-AlGaAs heterostructures was developed in the early 1970s, were the first wide-gap-emitter HBTs outperforming silicon transistors created at the Ioffe Institute. It was shown that the wide-gap emitter in a HBT not only prevents the amplification coefficient from falling at high injection levels, but also enables the whole set of parameters (especially the operation speed) of the transistors to be improved through the possible free choice of doping levels of the base and emitter regions. The possibility of controlling the flows of majority and minority carriers in heterostructures let to actualize a transistor with wide-gap emitter and collector, which furnished an opportunity to drastically improve the operating speed and reduce the saturation voltage of an HBT operating in a switching mode [190,191].

Microwave devices based on resonance-tunnel heterostructures and superlattices

Of growing interest for microwave applications are short-period superlattices in which ultrahigh operating frequencies have been achieved (up to several terahertz with frequency multiplication) and the active medium volumes are so large, as compared with double-barrier structures, that considerable microwave radiation power can be obtained. Here, much success has been achieved by researchers of the Ioffe Institute in cooperation with physicists from the University of Regensburg, Germany [192]. The key factor was the use of GaAs-AlAs and InGaAs-InAlAs superlattices with ultrathin (about monolayer thick) barriers. Extremely good results have been obtained with GaAs-AlAs superlattices with submonolayer AlAs barriers which are in fact structures with arrays of "anti"-quantum AlAs dots in a GaAs matrix.

Conclusion

Recently, impressing results have been obtained for short-wave radiation sources based on $A_{II}B_{VI}$ selenides and $A_{III}B_{V}$ nitrides. The use of heterostructure-related concepts and growth techniques developed for $A_{III}B_{V}$-based QDs and superlattices predetermined to a great extent the success of this research. A natural and predictable tendency is to apply heterostructure-related concepts and technological procedures to the new materials. The recently developed various $A_{III}B_{V}$, $A_{II}B_{VI}$, and $A_{IV}B_{VI}$ heterostructures substantiate this statement.

The classical heterostructures, QDs, and superlattices are already fairly perfect, and one can use quite a number of their unique properties. At the same time, structures with QWRs and QDs are still very young, and breathtaking discoveries and new unexpected applications are in store in this field. It is possible to say already now that ordered equilibrium QD arrays can be used in quite a number of devices: lasers, optical modulators, detectors and emitters for the far infrared, etc. Resonant tunneling via semiconductor atoms introduced into wider bandgap layers can improve device characteristics significantly. In a wider sense, QD structures are going to be developed both extensively and intensively. "Extensively" means new material systems capable of covering new regions of the energy spectrum. The system studied to the greatest extent—InGaAs-GaAs—has already been used to improve significantly characteristics of semiconductor lasers. It is likely that the problems related to the operation life of "green" and "blue" semiconductor lasers and even more general problems pertaining to fabrication of defect-free structures based on wide bandgap $A_{II}B_{VI}$ semiconductors and $A_{III}N$ nitrides can be solved by using QD structures in these systems.

"Intensively" assumes an understanding of the fact that the degree of ordering depends to a great extent on the exceedingly complicated growth conditions, material constants, and specific values of the surface free energy. The way to resonant-tunnel and single-electron devices and structures is an in-depth thorough study and evaluation of these parameters in order to achieve the maximum possible degree of ordering. On the whole, it is necessary to find more powerful mechanisms of self-organization to create ordered QD arrays. Correlated arrays of self-organized QWRs and QDs are rather promising for transverse Esaki–Tsu superlattices. Vertically coupled dots can be understood as a one-dimensional superlattice—an entirely novel object of study.

It is hardly possible to cover in a single paper even the main directions of the modern physics and technology of semiconductor heterostructures. Their number is much greater and the development of these directions will determine not only the prospects of solid state physics, but, in a sense, the future of the mankind.

The authors are grateful to D. Bimberg, V. Korol'kov, P. Kop'ev, A. Gorelenok, Yu. Zhilyaev, M. Mikhailova, V. Ustinov, A. Tsatsul'nikov, and Yu. Yakovlev for helpful discussions.

References

1. V. P. Zhuze and B. V. Kurchatov, *Zh. Eksp. Teor. Fiz.* (JETP) **2** 309 (1932).
2. Ya. I. Frenkel and A. F. Ioffe, *Phys. Zs. SU* Bd. 1, H. 1, 60 (1932).
3. Ya. I. Frenkel, *Phys. Rev.* **37** 17 (1931).
4. Ya. I. Frenkel, *Phys. Rev.* **37** 1276 (1931).
5. Ya. I. Frenkel, *Phys. Rev.* **37** 17 (1931).
6. E. F. Gross and N. A. Karriev, *Dok. Akad. Nauk* **84** 261 (1952).
7. E. F. Gross and N. A. Karriev, *Dok. Akad. Nauk* **84** 471 (1952).
8. B. I. Davydov, *Zh. Eksp. Teor. Fiz.* **9** 451 (1939).
9. N. H. Welker, *Zs. Naturforsch.* **7a** 744 (1952).
10. N. H. Welker, *Zs. Naturforsch.* **8a** 248 (1953).
11. N. A. Goryunova, *Thesis, Leningrad State University–Physico-Technical Inst.* 1951.
12. A. I. Blum, N. P. Mokrovskii and A. R. Regel, *Proc. VII Conf. on Semiconductors* (Kiev, 1950) [*Izv. AN SSSR. Ser. Phys.* **XVI** 139 (1952)].
13. W. Shokley, *US Patent 2569347*, September 25 (1951).
14. A. I. Gubanov, *Zh. Tekh. Fiz.* **20** 1287 (1950).
15. A. I. Gubanov, *Zh. Tekh. Fiz.* **21** 304 (1951).
16. H. Kroemer, *Proc. JRE* **45** 1535 (1957).
17. H. Kroemer, *RCA Rev.* **28** 332 (1957).
18. Zh. I. Alferov and R. F. Kazarinov, *Author's Certificate* No. 181737, Application No. 950840 with priority from March 30, 1963.
19. H. Kroemer, *Proc. IEEE* **51** 1782 (1963).
20. Zh. I. Alferov, V. B. Khalfin, and R. F. Kazarinov, *Sov. Phys.-Solid State* **8** 2480 (1967).
21. Zh. I. Alferov, *Sov. Phys. Semicond.* **1** 358 (1967).
22. L. Andreson, *IBM J. Res. Develop.* **4** 283 (1960).
23. L. Andreson, *Solid State Electron.* **5** 341 (1962).
24. Zh. I. Alferov, D. Z. Garbuzov, V. S. Grigor'ev, *et al.*, *Sov. Phys.-Solid State* **9** 208 (1967).
25. Zh. I. Alferov, Yu. V. Zhilyaev, and Yu. V. Shmartsev, *Sov. Phys. Semicond.* **5** 174 (1971).
26. Zh. I. Alferov, V. M. Andreev, V. I. Korol'kov, *et al.*, *Sov. Phys. Semicond.* **1** 1313 (1968).
27. H. S. Rupprecht, I. M. Woodall, and G. I. Pettit, *Appl. Phys. Lett.* **11** 81 (1967).
28. Zh. I. Alferov, V. M. Andreev, V. I. Korol'kov, *et al.*, *Sov. Phys. Semicond.* **2** 843 (1969).
29. Zh. I. Alferov, V. M. Andreev, V. I. Korol'kov, *et al.*, *Sov. Phys. Semicond.* **2** 1289 (1969).
30. Zh. I. Alferov, V. M. Andreev, V. I. Korol'kov, *et al.*, *Proc. IX ICPS*, Moscow, 23-29 July 1968, "Nauka", Leningrad, **1** 534 (1969).
31. Zh. I. Alferov, *Proc. Int. Conf. on Luminescemce* (Newark, Delaware USA, August 25-29), 1969.
32. Zh. I. Alferov, V. M. Andreev, V. I. Korol'kov, *et al.*, *Sov. Phys. Semicond.* **3** 460 (1969).
33. Zh. I. Alferov, *J. Luminesc.* **1** 2, 869 (1970).
34. Zh. I. Alferov, V. M. Andreev, E. L. Portnoi, *et al.*, *Sov. Phys. Semicond.* **3** 1107 (1970).
35. Zh. I. Alferov, V. M. Andreev, V. I. Korol'kov, *et al.*, *Sov. Phys. Semicond.* **3** 785 (1969).
36. Zh. I. Alferov, V. M. Andreev, M. V. Kagan, *et al.*, *Sov. Phys. Semicond.* **4** 2047 (1971).
37. Zh. I. Alferov, F. A. Ahmedov, V. I. Korol'kov, and V. G. Nikitin, *Sov. Phys. Semicond.* **7** 780 (1973).
38. Zh. I. Alferov, V. M. Andreev, V. I. Korol'kov, *et al.*, *Sov. Phys. Semicond.* **4** 481 (1970).
39. V. M. Andreev, L. M. Dolginov, and D. N. Tret'akov, *Liquid Phase Epitaxy in the Semiconductor Devices Technology* ed. Zh. I. Alferov, Moscow, Izd. "Sov. Radio" 328p., 1975.
40. R. R. Low, C. W. Mueller, J. I. Pankove, *et al.*, *Proc. IRE* **40** 1352 (1952).
41. Zh. I. Alferov, *Thesis, Leningrad, Physico-Technical Inst.* 1961.
42. H. Nelson, *RCA Rev.* **24** 603 (1963).
43. Zh. I. Alferov, N. Yu. Antonishkis, I. N. Arsent'ev, *et al.*, *Sov. Phys. Semicond.* **21** 162 (1987).
44. Zh. I. Alferov, A. T. Gorelenok, and D. Z. Garbuzov, *Sov. Techn. Phys. Lett.* **8** 113 (1982).
45. A. A. Andaspaeva, A. P. Guseynov, and A. N. Baranov, *Fiz. Tekhn. Poluprovodn.* **24** 1708 (1990).
46. Zh. I. Alferov, V. M. Andreev, S. G. Konnikov, *et al.*, *Kristall und Technik* **11** 1013 (1976).
47. Zh. I. Alferov, V. M. Andreev, D. Z. Garbuzov, *et al.*, *Pisma Zh. Tekhn. Fiz.* **48** 809 (1978).
48. V. M. Andreev, A. B. Kazantsev, V. R. Larionov, *et al.*, *AIP Conf. Proc.* Ed: Zh. I. Alferov, **240** 24 (1991).
49. V. M. Andreev, L. B. Karlina, A. B. Kazansev, *et al.*, *Proc. of the First World Conf. on Photovoltaic Energy Conversion*, Hawaii, USA, 1713 (1994).
50. Zh. I. Alferov, M. Z. Zhingarev, S. G. Konnikov, *et al.*, *Sov. Phys. Semicond.* **16** 532 (1982).
51. N. N. Ledentsov, D. Bimberg, Yu. M. Shernyakov, *et al.*, *Appl. Phys. Lett.* **70** 2888 (1997).
52. Zh. I. Alferov, N. Yu. Gordeev, S. V. Zaitsev, *et al.*, *Sov. Phys. Semicond.* **30** 197 (1996).
53. D. A. Vinokurov, V. M. Lantratov, M. A. Sinitsin, *et al.*, *Sov. Phys. Semicond.* **25** (1991).
54. V. M. Andreev, V. V. Komin, I. V. Kochnev, *et al.*, *Proc. Fist World Conf. on Photovoltaic Energy Conversion*, Hawaii, vol. II, p. 1894, 1994.
55. P. S. Kop'ev and N. N. Ledentsov, *Sov. Phys. Semicond.* **22** 1093 (1988) and references in this paper.
56. R. Heckingbottom, C. J. Todd, and G. J. Davies, *J. Electrochem. Soc.* **127** 444 (1980).
57. R. Heckingbottom and G. Davies, *J. Cryst. Growth* **50** 644 (1980).
58. S. V. Ivanov, P. S. Kop'ev, and N. N. Ledentsov, *J. Cryst. Growth* **104** 345 (1990).
59. S. V. Ivanov, P. S. Kop'ev, and N. N. Ledentsov, *J. Cryst. Growth* **108** 661 (1990).
60. S. V. Ivanov, P. S. Kop'ev, and N. N. Ledentsov, *J. Cryst. Growth* **111** 151 (1991).
61. S. V. Ivanov, A. A. Boudza, R. N. Kutt, *et al.*, *J. Cryst. Growth* **156** 191 (1995).
62. A. Yu. Egorov, A. R. Kovsh, A. E. Zhukov, *et al.*, *Phys. Semicond.* **31** 989 (1997).
63. Zh. I. Alferov, V. M. Andreev, S. G. Konnikov, *et al.*, *Proc. Int. Conf. on Physics and Chemistry of Semiconductor Heterojunctions and Layer Structures* (Budapest, October 1970) [*Academiai Kiado*, **1**, 93 (1971)].
64. G. A. Antipas, R. L. Moon, and J. W. James, *Conf. Ser. IOP* **17** 48 (1973).
65. L. James, G. Antipas, and R. Moon, *Appl. Phys. Lett.* **22** 270 (1973).
66. A. P. Bogatov, L. M. Dolginov, and L. V. Drughinina, *Kvant. Electron.* **1** 2294 (1974).
67. J. J. Hsieh, *Appl. Phys. Lett.* **28** 283 (1976).
68. Zh. I. Alferov, I. N. Arsent'ev, and D. Z. Garbuzov, *Sov. Techn. Phys. Lett.* **1** 147 (1975).
69. Zh. I. Alferov, F. A. Ahmedov, and V. I. Korol'kov, *Sov. Techn. Phys. Lett.* **1** 191 (1975).
70. W. R. Hitchens, N. Holonyak Jr., and P. D. Wright, *Appl. Phys. Lett.* **27** 245 (1975).
71. H. Kroemer and G. Griffiths, *IEEE Electron. Dev. Lett.* **EDL-4** 20 (1983).
72. Zh. I. Alferov, D. Z. Garbuzov, E. P. Morozov, and E. L. Portnoy, *Sov. Phys. Semicond.* **3** 885 (1969).

73. A. N. Baranov, B. E. Dzhurtanov, A. N. Imenkov, *et al.*, *Sov. Phys. Semicond.* **20** 1385 (1986).
74. V. N. Lutskii, *Phys. Stat. Sol. (a)* **1** 199 (1970).
75. V. N. Lutskii and L. A. Kulik, *Pisma Zh. Eksp. Teor. Fiz.* **8** 3 (1968).
76. L. V. Keldysh, *Fiz. Tverd. Tela* **4** 2265 (1962).
77. R. Davies and H. Hosack, *J. Appl. Phys.* **33** 864 (1963).
78. L. V. Iogansen, *Zh. Eksp. Teor. Fiz.* **45** 207 (1963).
79. L. Esaki and R. Tsu, *IBM J. Res. Develop.* **14** 61 (1970).
80. R. F. Kazarinov and R. A. Suris, *Sov. Phys. Semicond.* **5** 707 (1971).
81. R. F. Kazarinov and R. A. Suris, *Sov. Phys. Semicond.* **5** 120 (1972).
82. L. L. Chang, L. Esaki, and R. Tsu, *Appl. Phys. Lett.* **24** 593 (1974).
83. J. Faist, F. Capasso, D. L. Sivco, *et al.*, *Science* **264** 553 (1994).
84. R. Dingle, W. Wiegmann, and C. H. Henry, *Phys. Rev. Lett.* **33** 827 (1974).
85. R. Dingle, H. L. Störmer, A. C. Gossard, and W. Wiegmann, *Appl. Phys. Lett.* **33** 665 (1978).
86. D. C. Tsui, H. L. Störmer, and A. C. Gossard, *Phys. Rev. Lett.* **48** 1559 (1982).
87. J. W. Matthews and A. E. Blakeslee, *J. Cryst. Growth* **32** 265 (1976).
88. G. C. Osbourn, *J. Appl. Phys.* **53** 1586 (1982).
89. A. I. Ekimov and A. A. Onushenko, *Pisma Zh. Eksp. Teor. Fiz.* **34** 363 (1981).
90. Al. L. Efros and A. L. Efros, *Sov. Phys. Semicond.* **16** 772 (1982).
91. S. P. Beamount, *Low-Dimensional Structures in Semiconductors*, ed. A. R. Peaker and H. G. Grimmeiss, Plenum Press, New York, p. 109, 1991.
92. E. Kapon, M. C. Tamargo, and D. M. Hwang, *Appl. Phys. Lett.* **50** 347 (1987).
93. H. Haken, *Synergetics*, Springer, Berlin-Heidelberg, 1977.
94. I. P. Ipatova, V. G. Malyshkin, and V. A. Shchukin, *J. Appl. Phys.* **74** 7198 (1993).
95. V. I. Marchenko, *JETP* **54** 605 (1981).
96. A. F. Andreev and Yu. A. Kosevich, *Zh. Eksp. Teor. Fiz.* **81** 1435 (1981).
97. V. I. Marchenko and A. Ya. Parshin, *Zh. Eksp. Teor. Fiz.* **79** 257 (1980).
98. V. A. Shchukin, N. N. Ledentsov, P. S. Kop'ev, and D. Bimberg, *Phys. Rev. Lett.* **75** 2968 (1995).
99. Zh. I. Alferov, D. Bimberg, A. Yu. Egorov, *et al.*, *Usp. Fiz. Nauk* **165** 224 (1995).
100. P. D. Wang, N. N. Ledentsov, C. M. Sotomayor Torres, *et al.*, *Appl. Phys. Lett.* **64** 1526 (1994).
101. P. D. Wang, N. N. Ledentsov, C. M. Sotomayor Torres, *et al.*, *Appl. Phys. Lett.* **66** 112 (1995).
102. V. Bressler-Hill, A. Lorke, S. Varma, *et al.*, *Phys. Rev. B* **50** 8479 (1994).
103. J. M. Moison, F. Houzay, F. Barthe, *et al.*, *Appl. Phys. Lett.* **64** 196 (1994).
104. D. Leonard, M. Krishnamurthy, C. M. Reaves, *et al.*, *Appl. Phys. Lett.* **63** 3203 (1993).
105. N. N. Ledentsov, M. Grundmann, N. Kirstaedter, *et al.*, *Proc. 22nd Int. Conf. Phys. Semicond.*, Vancouver, Canada, August 1994, ed. D. J. Lockwood, World Scientific, Singapore, Vol. 3, p. 1855, 1994.
106. M. Grundmann, J. Christen, N. N. Ledentsov, *et al.*, *Phys. Rev. Lett.* **74** 4043 (1995).
107. N. N. Ledentsov, V. M. Ustinov, S. V. Ivanov, *et al.*, *Usp. Fiz. Nauk* **166** 423 (1996).
108. N. N. Ledentsov, *Proc. of the 23rd Int. Conf. on the Physics of Semiconductors*, Berlin, Germany, July 21–26, 1996, ed. M. Scheffler and R. Zimmermann (World Scientific, Singapoure), v. 1, p. 19, 1996.
109. N. N. Ledentsov, M. Grundmann, N. Kirstaedter, *et al.*, *Proc. of the 7th Int. Conf. on Modulated Semiconductor Structures*, Madrid, 10–14 July, 1995, *Solid State Electron.* **40** 785 (1996).
110. R. Heitz, M. Grundmann, N. N. Ledentsov, *et al.*, *Appl. Phys. Lett.* **68** 361 (1996).
111. S. Ruvimov, Z. Liliental-Weber, N. N. Ledentsov, *et al.*, *Mat. Res. Soc. Symp. Proc.* Vol. 421, eds. by: R. J. Shul, S. J. Pearton, F. Ren, C.-S. Wu, Pittsburgh, PA, p. 383, 1996.
112. Zh. I. Alferov, N. A. Bert, A. Yu. Egorov, *et al.*, *Phys. Semicond.* **30** 194 (1996).
113. N. N. Ledentsov, J. Bohrer, D. Bimberg, *et al.*, *Mat. Res. Soc. Symp. Proc.* Vol. 421, eds.: R. J. Shul, S. J. Pearton, F. Ren, C.-S. Wu, Pittsburgh, p. 133, 1996.
114. N. N. Ledentsov, V. A. Shchukin, M. Grundmann, *et al.*, *Phys. Rev. B* **54** 8743 (1996).
115. F. Hatami, N. N. Ledentsov, M. Grundmann, *et al.*, *Appl. Phys. Lett.* **67** 656 (1995).
116. I. Hayashi, *IEEE Trans. Electron. Dev.* **ED-31** 1630 (1984).
117. Zh. I. Alferov, V. M. Andreev, D. Z. Garbuzov, and Yu. V. Zhilyaev, *Sov. Phys. Semicond.* **4** 1573 (1971).
118. I. Hayashi, M. B. Panish, P. W. Foy, *et al.*, *Appl. Phys. Lett.* **17** 109 (1970).
119. Zh. I. Alferov, V. M. Andreev, R. F. Kazarinov, *et al.*, *Author's Certificate No. 392875*, Application No. 1677436 with priority from July 19, 1971.
120. H. Kogelnik and C. V. Shank, *Appl. Phys. Lett.* **18** 152 (1971).
121. R. F. Kazarinov and R. A. Suris, *Sov. Phys. Semicond.* **6** 1184 (1973).
122. Zh. I. Alferov, S. A. Gurevich, R. F. Kazarinov, *et al.*, *Sov. Phys. Semicond.* **8** 541 (1974).
123. Zh. I. Alferov, S. A. Gurevich, N. V. Klepnikova, *et al.*, *Sov. Techn. Phys. Lett.* **1** 286 (1975).
124. M. Nakamura, A. Yariv, H. W. Yen, S. Somekh, *et al.*, *Appl. Phys. Lett.* **22** 315 (1973).
125. D. R. Scifres, R. D. Burnham, W. Streifer, *et al.*, *Appl. Phys. Lett.* **25** 203 (1974).
126. S. A. Gurevich, S. Yu. Karpov, E. L. Portnoy, *et al.*, *Pisma Zh. Tekhn. Fiz.* **12** 268 (1986).
127. J. P. van der Ziel, R. Dingle, R. C. Miller, *et al.*, *Appl. Phys. Lett.* **26** 463 (1975).
128. R. D. Dupuis, P. D. Dapkus, N. Holonyak Jr., *et al.*, *Appl. Phys. Lett.* **32** 295 (1978).
129. W. T. Tsang, *Appl. Phys. Lett.* **40** 217 (1982).
130. E. Rezek, H. Shichijo, B. A. Vojak, and N. Holonyak Jr., *Appl. Phys. Lett.* **31** 534 (1977).
131. Zh. I. Alferov, D. Z. Garbuzov, I. N. Arsent'ev, *et al.*, *Sov. Phys. Semicond.* **19** 679 (1985).
132. Zh. I. Alferov, V. M. Andreev, A. A. Vodnev, *et al.*, *Sov. Techn. Phys. Lett.* **12** 450 (1986).
133. Zh. I. Alferov, D. Z. Garbuzov, S. V. Zaitsev, *et al.*, *Sov. Phys. Semicond.* **21** 914 (1987).
134. Zh. I. Alferov, N. Yu. Antonishkis, I. N. Arsent'ev, *et al.*, *Sov. Phys. Semicond.* **22** 650 (1988).
135. D. Z. Garbuzov, *et al.*, *Technical Digest CLEO*, paper THU44, 396 (1988).
136. D. Z. Garbuzov, *et al.*, *Conf. Digest 12th Int. Semicond. Laser Conf.* (Davos, Switzerland, 1990) p. 238.
137. Zh. I. Alferov, A. M. Vasiliev, S. V. Ivanov, *et al.*, *Pisma Zh. Tekhn. Fiz.* **14** 1803 (1988).
138. Y. Arakawa and H. Sakaki, *Appl. Phys. Lett.* **40** 939 (1982).
139. S. Simhony, E. Kapon, T. Colas, *et al.*, *Appl. Phys. Lett.* **59** 2225 (1991).
140. N. N. Ledentsov, V. M. Ustinov, A. Yu. Egorov, *et al.*, *Phys. Semicond.* **28** 832 (1994).
141. N. Kirstaedter, N. N. Ledentsov, M. Grundmann, *et al.*, *Electron. Lett.* **30** 1416 (1994).
142. N. Kirstaedter, O. G. Schmidt, N. N. Ledentsov, *et al.*, *Appl. Phys. Lett.* **69** 1226 (1996).
143. D. Bimberg, N. Kirstaedter, N. N. Ledentsov, *et al.*, *IEEE J. of Selected Topics in Quantum Electronics* **3** 196 (1997).
144. L. V. Asryan and R. A. Suris, *Semicond. Sci. Technol.* **11** 554 (1996).
145. L. V. Asryan and R. A. Suris, *IEEE Journal of Selected Topics in Quantum Electronics* **3** 148 (1997).
146. M. Grundmann and D. Bimberg, *Jpn. J. Appl. Phys.* **36** Part I, 4181 (1997).
147. M. Grundmann and D Bimberg, *Phys. Rev. B* **55** 9740 (1997).
148. H. Saito, K. Nishi, I. Ogura, S. Sugou, and Y. Sugimoto, *Appl. Phys. Lett.* **69** 3140 (1996).

149. J. A. Lott, N. N. Ledentsov, V. M. Ustinov, *et al.*, *Electronics Lett.* **33** 1150 (1997).
150. N. N. Ledentsov, I. L. Krestnikov, M. V. Maximov, *et al.*, *Appl. Phys. Lett.* **69** 1343 (1996), ibid. **70** 2766 (1997).
151. L. A. Graha, Q. Deng, D. G. Deppe, and D. L. Huffaker, *Appl. Phys. Lett.* **70** 814 (1997).
152. C. H. McMahon, J. W. Bae, C. S. Menonui, *et al.*, *Appl. Phys. Lett.* **66**, 2171 (1995).
153. L. E. Vorob'ev, D. A. Firsov, V. A. Shal'gin, *et al.*, *Pisma Zh. Tekhn. Fiz.* **67** 256 (1998).
154. G. E. Cirlin, V. N. Petrov, V. G. Dubrovskii, *et al.*, *Pisma Zh. Tekhn. Fiz.* **24** 10 (1988).
155. Zh. I. Alferov, V. M. Andreev, D. Z. Garbuzov, and V. D. Rumyantsev, *Sov. Phys. Semicond.* **9** 462 (1975).
156. A. Abdulaev, V. G. Agafonov, V. M. Andreev, *et al.*, *Sov. Phys. Semicond.* **11** 272 (1977).
157. Zh. I. Alferov, V. M. Andreev, D. Z. Garbuzov, *et al.*, *Sov. Phys. Semicond.* **8** 2350 (1974).
158. Zh. I. Alferov, V. M. Andreev, D. Z. Garbuzov, *et al.*, *Sov. Techn. Phys. Lett.* **45** 368 (1975).
159. Zh. I. Alferov, V. M. Andreev, D. Z. Garbuzov, *et al.*, *Sov. Techn. Phys. Lett.* **3** 657 (1977).
160. Zh. I. Alferov, V. M. Andreev, D. Z. Garbuzov, *et al.*, *Sov. Techn. Phys. Lett.* **4** 241 (1978).
161. A. A. Andaspaeva, A. P. Guseynov, A. N. Baranov, *et al.*, *Pisma Zh. Tekhn. Fiz.* **15** 71 (1989).
162. A. A. Popov, V. V. Sherstnev, and Yu. P. Yakovlev, *Techn. Phys. Lett.* **23** 701 (1997).
163. A. A. Popov, M. V. Stepanov, V. V. Sherstnev, and Yu. P. Yakovlev, *Techn. Phys. Lett.* **23** 828 (1997).
164. M. Aidaraliev, N. V. Zotova, S. A. Karandashov, *et al.*, *Phys. Stat. Sol. (a)* **115** k117, (1989).
165. Zh. I. Alferov, V. M. Andreev, N. S. Zimogorova, and D. N. Tretyakov, *Sov. Phys. Semicond.* **3** 1633 (1969).
166. V. M. Andreev, T. M. Golovner, M. B. Kagan, *et al.*, *Sov. Phys. Semicond.* **3** 2289 (1973).
167. Zh. I. Alferov, V. M. Andreev, D. Z. Garbuzov, *et al.*, *Sov. Phys. Semicond.* **11** 1765 (1977).
168. V. M. Andreev, V. P. Khvostikov, E. V. Paleeva, *et al.*, *Proc. of the 25th IEEE Photovoltaic Specialists Conf.* Washington, USA, p. 143, 1996
169. V. M. Andreev, V. S. Kalinovsky, and V. V. Komin, *et al.*, *Proc. of the 4th European Space Power Conf.* Poitiers, France, 1995.
170. L. M. Fraas, J. E. Avery, J. Martin, *et al.*, *IEEE Trans. Electron Dev.* **37** 444 (1990).
171. V. M. Andreev, L. B. Karlina, V. P. Khvostikov, *et al.*, *Proc. of the 13th European Photovoltaic Solar Energy Conf.* Nice, France, p. 329, 1995.
172. K. A. Bertness, S. R. Kurtz, D. J. Friedman, *et al.*, *Appl. Phys. Lett.* **65** 989 (1994).
173. M. Yamaguchi and S. Wakamatsu, *Proc. of the 25th IEEE Photovoltaic Specialists Conf.*, Washington, USA, p. 9, 1996.
174. V. M. Andreev, V. P. Khvostikov, E. V. Paleeva, *et al.*, *Proc. of the 23d Int. Symp. of Compound Semiconductors* St. Petersburg, Russia, p. 425, 1996.
175. M. Z. Zhingarev, V. I. Korol'kov, M. P. Mikhailova, *et al.*, *Sov. Techn. Phys. Lett.* **5** 355 (1979).
176. L. A. Volkov, V. G. Danil'chenko, and V. I. Korol'kov, *Sov. Techn. Phys. Lett.* **14** 682 (1988).
177. A. T. Gorelenok, *Photodetectors and Photoconverters* Leningrad, Nauka p. 37–63, (in Russian) 1986.
178. V. M. Andreev, A. T. Gorelenok, M. Z. Zhingarev, *et al.*, *Pisma Zh. Tekhn. Fiz.* **55** 668 (1985).
179. I. A. Andreev, M. A. Afrailov, A. N. Baranov, *et al.*, *Sov. Techn. Phys. Lett.* **15** 15 (1989).
180. I. A. Andreev, A. N. Baranov, M. P. Mikhailova, *et al.*, *Sov. Techn. Phys. Lett.* **18** 50 (1992).
181. M. P. Mikhailova, S. V. Slobodchikov, N. D. Stoyanov, *et al.*, *Sov. Techn. Phys. Lett.* **22** 642 (1996).
182. A. P. Dmitriev, M. P. Mikhailova, and I. N. Yassievich, *Phys. Stat. Sol. (b)* **140** 9 (1987).
183. I. A. Andreev, M. A. Afrailov, A. N. Baranov, *et al.*, *Sov. Techn. Phys. Lett.* **14** 435 (1988).
184. Zh. I. Alferov, Ya. V. Bergmann, V. I. Korol'kov, *et al.*, *Sov. Phys. Semicond.* **12** 38 (1978).
185. Zh. I. Alferov, V. I. Korol'kov, N. Rahimov, *et al.*, *Sov. Phys. Semicond.* **12** 42 (1978).
186. V. I. Korol'kov, V. S. Yuferev, and A. A. Yakovenko, *Sov. Phys. Semicond.* **14** 1005 (1978).
187. V. I. Korol'kov, A. S. Prokhorenko, and A. V. Porkov, *Sov. Phys. Semicond.* **18** 311 (1992).
188. Yu. M. Zadiranov, V. I. Korol'kov, S. I. Ponomarev, *et al.*, *Sov. Techn. Phys. Lett.* **32** 466 (1987).
189. Zh. I. Alferov, V. M. Efanov, Yu. M. Zadiranov, *et al.*, *Sov. Techn. Phys. Lett.* **12** 529 (1986).
190. Zh. I. Alferov, F. A. Akhmedov, and V. I. Korol'kov, *Sov. Techn. Phys. Lett.* **1**, 769 (1975).
191. Zh. I. Alferov, G. D. Andreev, V. I. Korol'kov, *et al.*, *Sov. Phys. Semicond.* **7** 621 (1973).
192. E. Schomburg, J. Grenzer, K. Hofbeck, *et al.*, *IEE J. Selected Topics in Quantum. Electron.* **2** 724 (1996).